UNIVERSITY OF CALGARY

FEASIBILITY OF UTILIZING ON-SITE SOLAR THERMAL ENERGY PRODUCTION PLUS THERMAL ENERGY STORAGE FOR EV CHARGING

by

Ian Choveaux

A RESEARCH PROJECT SUBMITTED

IN PARTIAL FULFILMENT OF THE REQUIREMENTS FOR THE

DEGREE OF MASTER OF SCIENCE

GRADUATE PROGRAM IN SUSTAINABLE ENERGY DEVELOPMENT

CALGARY, ALBERTA

AUGUST, 2021

ABSTRACT

This paper seeks to determine the feasibility of utilizing on-site concentrated solar power plus thermal energy storage to produce energy for electric vehicle charging in Medicine Hat, Alberta. A literature review outlines system specifications to determine the potential viability of a novel concentrated solar power generation technology through an assessment of the solar thermoelectricity via advanced latent heat storage (STEALS) system which utilizes miscibility gap alloys (MGAs) as the thermal energy storage component of the system. A comparative economic analysis that utilized the U.S. National Renewable Energy Lab's (NREL) System Advisor Model (SAM) to determine the levelized cost of energy (LCOE) and resultant feasibility of a project or system, found a solar photovoltaic plus STEALS system to have a lower LCOE than a solar photovoltaic plus battery energy storage system.

ACKNOWLEDGEMENTS

I would like to thank my supervisor, Ganesh Doluweerawatta Gamage, for your patience, understanding, support and guidance throughout this process. Thank you for sharing your time and knowledge in completion of this project.

Thank you to Erich Kisi, for providing information and guidance regarding miscibility gap alloys, and to Dr. David Wood for connecting me with Erich Kisi.

Thank you to my family, in particular my wife, for your unwavering love, support and understanding throughout the pursuit of my Masters.

Lastly, thank you to my fellow SEDV 'covid cohort', which provided an immense amount of support, compassion, engagement and fun in completion of our studies. Our shared experience has left an indelible mark on me.

TABLE OF CONTENTS

LIST OF TABLES

LIST OF FIGURES

LIST OF ABBREVIATIONS

bbl barrel of oil

BESS battery energy storage system

BEV battery electric vehicle

°C degrees Celsius

CO^2_e carbon dioxide equivalent

CSP concentrated solar power

EROCI energy return on capital invested

EV electric vehicles

GW gigawatt

ICE internal combustion engine

IPCC Intergovernmental Panel on Climate Change

J joule

kW kilowatt

kW/m^2 kilowatts per square meter

$kWh/m^2/day$ kilowatt hours per square meter per day

kWh kilowatt hour

LCOE levelized cost of energy

MGA miscibility gap alloys

Mt CO2 eq megatonnes of carbon dioxide equivalent

MW megawatt

MW_e megawatt equivalent

NREL National Renewable Energy Lab

PCM phase change material

PSH pumped storage hydropower

SAM System Advisor Model

SiC silicon carbide

Solar PV solar photovoltaic

STEALS solar thermoelectricity via advanced latent heat storage

tCO_{2e}/MWh tonnes of carbon dioxide equivalent per megawatt hour of energy produced

TEG thermoelectric generator

TES thermal energy storage

UNSDGs United Nations Sustainable Development Goals

VRE variable renewable energy

W/cm^3 watts per cubic centimeter

W/m/K watts per meter per degree Kelvin

CHAPTER 1: INTRODUCTION

As the recently released Intergovernmental Panel on Climate Change (IPCC) report made clear, rapid decarbonization of energy systems is required if we are to stave off the worst impacts of climate change (Masson-Delmotte, et al., 2021). As transportation accounts for 25% of Canada's emissions, cleaner transportation options can play a crucial role in meeting this goal (Environment and Climate Change Canada, 2021; Government of Canada, 2021). To maximize the environmental and health benefits derived from the expected mass-scale adoption of electric vehicles, inexpensive, non-emitting forms of power generation and energy storage should be pursued (Murphy, et al., 2021).

The transportation sector is undergoing a period of rapid transformation. In the next few years, a massive influx of new electric vehicles is expected to take place in markets around the world. In fact, in some more established markets, electric vehicles already make up the majority of new car sales (Edelstein, 2021). From an initial baseline of 7.9 million electric vehicles on the road in 2020, projections indicate that over the next five years, more than 50 million electric vehicles (EVs) are expected to be on the road, with numbers increasing to 130 million electric vehicles, globally, by 2030 and ultimately over 1.1 billion EVs by 2050 (IRENA, 2020, p. 40; Hoover, Nägele, Polymeneas, & Sah, 2021).

As the federal government has recently announced a ban on the sale of internal-combustion engine (ICE) vehicles by 2035 to align with the goals of a decarbonized transportation sector (Clean Energy Canada, 2021a; Scherer, 2021), considerations must be undertaken for how to accommodate the increased demand on our electricity grid (Dao, 2021; Alberta Electric System Operator, 2021; Alexander, Crisostomo, Krell, Lu, & Ramesh, 2021; Coignard, Saxena, Greenblatt, & Wang, 2018; Murphy, et al., 2021).

To accommodate this mass influx of EVs, between $110-$180 billion will be required to deploy the requisite charging infrastructure between 2020 and 2030 (Hoover, Nägele, Polymeneas, & Sah, 2021). Previous research has shown that oil will require a long-term breakeven price of between $10-$20/bbl to remain competitive for mobility (Lewis, 2019). Even then, the infrastructure required to provide the same amount of mobility (measured as power at the wheels) will be significantly less (6.2x-7x less) given a shift to electric vehicles on a renewable energy powered grid, as compared to internal combustion vehicles powered by fossil fuels (Lewis, 2019).

Figure 1 - EROCI of Capital - Renewables & EVs versus Gasoline

ENERGY AND TECHNOLOGY SOURCES	GROSS POTENTIAL ENERGY[5]	GROSS ENERGY PURCHASED[6]	GROSS ENERGY AT PUMP OR CHARGER[7]	NET EROCI (MOBILITY)[8]	MULTIPLE OF EROCI OF OIL AT $60/BBL	IMPLIED OIL PRICE FOR SAME NET EROCI
Oil for gasoline LDVs	2,824TWh	1,497TWh	1,347TWh	270TWh	1x	$60/bbl
Onshore wind w/EVs	3,443TWh	2,583TWh	2,324TWh	1,673TWh	6.2x	$9.7/bbl
Offshore wind w/EVs	3,871TWh	2,903TWh	2,613TWh	1,881TWh	7x	$8.6/bbl
Solar-PV w/EVs	3,249TWh	2,437 Wh	2,315TWh	1,667TWh	6.2x	$9.7/bbl

Source: BNP Paribas Asset Management *In this report, net EROCI is the amount of mobility bought for a given capital outlay.

(Note: Lewis, 2019)

Figure 2 - EROCI of Capital - Renewables & EVs versus Diesel

ENERGY AND TECHNOLOGY SOURCES	GROSS POTENTIAL ENERGY	GROSS ENERGY PURCHASED	GROSS ENERGY AT PUMP OR CHARGER	NET EROCI (MOBILITY)	MULTIPLE OF EROCI OF OIL AT $60/BBL	IMPLIED OIL PRICE FOR SAME NET EROCI
Oil for diesel vehicles	2,824TWh	1,497TWh	1,497TWh	524TWh	1x	$60/bbl
Onshore wind w/EVs	3,443TWh	2,583TWh	2,324TWh	1,673TWh	3.2x	$16.7/bbl
Offshore wind w/EVs	3,871TWh	2,903TWh	2,613TWh	1,881TWh	3.6x	$18.8/bbl
Solar-PV w/EVs	3,249TWh	2,437TWh	2,315TWh	1,667TWh	3.2x	$18.9/bbl

Source: BNP Paribas Asset Management *In this report, net EROCI is the amount of mobility bought for a given capital outlay.

(Note: Lewis, 2019)

Though overall capital costs are expected to be drastically less under a renewable energy powered system, other factors must be considered. Demand management and grid stability will be critical components of mass adoption of electric vehicles. Studies have shown that demand related to the charging needs of just 10 million EVs would require an additional 3GW of power, if all vehicles were charged simultaneously, versus an increase of only 0.5GW, if smart charging is incentivized (IRENA, 2020, p. 40). Clearly, smarter energy systems will be required in order to handle this mass influx of EVs (Alberta Electric System Operator, 2021; Alexander, Crisostomo, Krell, Lu, & Ramesh, 2021; Coignard, Saxena, Greenblatt, & Wang, 2018).

The objective of this research is to determine if it is technically feasible to generate enough energy from on-site solar power production to enable electric vehicle charging. This research will contribute to the design of a sustainable operating model for greenfield construction and/or the transition and retrofitting of existing fueling stations, to accommodate EV charging applications as the global vehicle fleet transitions from internal-combustion engine (ICE) vehicles. Though focused on a singular location, the resulting research and design scheme may serve as a blueprint or prototype for such systems in other locations.

This research will address UNSDGs 7 - Affordable & Clean Energy; 9 - Industry, Innovation & Infrastructure; 11 - Sustainable Cities & Communities (United Nations, n.d.), along the themes of energy, environment and technological feasibility and will serve to demonstrate the potential of the electrification of transport, powered by renewable energy sources to achieve economy wide decarbonization, while showcasing the economic development potential of cleaner energy technologies (Doluweera, 2020a). To achieve this aim, the research will assess the viability of a system that utilizes a novel combined concentrated solar power (CSP) and thermal energy storage (TES) system to determine optimal system dynamics and operability within the Alberta context. The system being considered includes two new technologies: a novel phase-change material, miscibility gap alloys, are assessed as the thermal energy storage medium, housed within a solar thermoelectricity via advanced latent heat storage (STEALS) module which uses a heliostat array as a heat source. The heat that is generated from the heliostat field is concentrated on the STEALS module to generate electricity that is then used to charge electric vehicles.

CHAPTER 2: LITERATURE REVIEW

The transition from internal-combustion engine (ICE) vehicles to electric vehicles (EV) in the personal mobility market is informed by a number of factors. Despite studies indicating that electric vehicles could meet the daily requirements of the majority of drivers, range anxiety related to the perceived inability to travel long distances and challenges related the time it takes to recharge EVs are a limiting factor in EV adoption (Needell, McNerney, Chang, & Trancik, 2016).

Difficulties in finding a charging station are also a concern for prospective purchasers concerned about the lack of available charging infrastructure (KPMG, 2021). Such challenges will be mitigated as the EV charging infrastructure network continues to build out and additional services become available to make EV charging simpler, and more seamless. Integrating smart charging to "shift the timing of charging based on electricity pricing, carbon intensity, demand response, or other grid signals" (Alexander, Crisostomo, Krell, Lu, & Ramesh, 2021, p. 57) can mitigate these concerns, ensuring that driver's range requirements and preferred travel times are met (Alexander, Crisostomo, Krell, Lu, & Ramesh, 2021). With major announcements of continued development of EV charging systems by oil majors, including Shell, targeting at least 500,000 additional EV charging stations within their network in the next five years, as well as indications that the US will be introducing a nationwide EV charging network of similar scale, determining the most suitable system design for infrastructure will be of utmost importance (Kane, 2021; Evannex, 2021). Additional resources including websites such as PlugShare and new features offered by Google Maps make finding EV charging stations simple and straightforward, offering additional benefits of ease, convenience and timesaving for EV drivers in locations where such services are available (PlugShare, 2021a; Donaldson, 2019).

Continued advancements in battery technology and economies of scale should enable BEVs (battery electric vehicles) to reach cost parity with conventional (ICE – internal combustion engine) vehicles across most vehicle segments within the next five to ten years (Lutsey & Nicholas, 2019). As battery technology has made marked improvements over the last decade, production costs for electric vehicles have also experienced substantial cost declines, leading to greater appetite from and opportunity for auto manufacturers to produce such vehicles (Clean Energy Canada, 2021; Sharpe, Lutsey, Smith, & Kim, 2020). Rapid cost declines of 89% over the last decade have led to projections indicating that electric vehicles are expected to reach a purchase price parity with internal combustion engine vehicles within the next five years (Henze, 2020; Lutsey & Nicholas, 2019). The total cost of operations of electric vehicles has been indicated to be just a fraction of that for comparable internal combustion engine vehicles, owing to lower maintenance and fueling costs, making the switch to electric vehicles that much more enticing to prospective buyers (Harto, 2020). As total cost of ownership is projected to be lower for BEVs across most vehicle segments, and as consumer attitudes toward EV adoption improve (KPMG, 2021), additional policy supports continue to drive innovation and a transition towards electrification of transport (Transport Canada, 2020). Such policy supports will be important as recent consumer surveys indicate a majority of consumers intend to opt for an electric vehicle with their next vehicle purchase, though these findings are largely contingent upon there being rebates and incentives offered as part of the purchase (KPMG, 2021). The recent announcement of the ban on fossil fueled powered vehicles in Canada by 2035 (Clean Energy Canada, 2021a; Scherer, 2021) should be attainable, providing Canada an opportunity to play a leadership role in developing new battery technology (Clean Energy Canada, 2021; Sharpe, Lutsey, Smith, & Kim, 2020). An integrated North American vehicle emissions strategy coupled with renewed interest and appetite from automakers and supportive incentives for consumers should help foster conditions conducive to greater market penetration of electric vehicles.

There are some concerns regarding the grid's ability to handle the mass influx of electric vehicles (Dao, 2021; Alberta Electric System Operator, 2021), though these forecasts do not include the potential for vehicle-to-grid, or smart-charging charging and additional storage capacity enabled by mass-scale adoption of EVs to reduce overall system demand, (Coignard, Saxena, Greenblatt, & Wang, 2018; Alexander, Crisostomo, Krell, Lu, & Ramesh, 2021; U.S. Department of Energy, 2020; Murphy, et al., 2021). A transportation system in which renewable energy generation is combined with electrified mobility options is not only significantly cheaper to build and operate (Lewis, 2019), EVs can provide additional storage capacity (U.S. Department of Energy, 2020) which can defer investments in new generating capacity (Coignard, Saxena, Greenblatt, & Wang, 2018; Murphy, et al., 2021) and transmission lines, leading to increased cost savings while helping reduce emissions (Doluweera, Hahn, Bergerson, & Pruckner, 2020; Knobloch, et al., 2020; Murphy, et al., 2021). Smart charging can align charging times with periods when wind and solar energy are abundant helping to better aid in renewable energy integration by reducing curtailment and maximizing use of renewable energy sources, saving drivers money and reducing emissions (Alexander, Crisostomo, Krell, Lu, & Ramesh, 2021). Further, there is significant potential of increasing storage capacity by enabling bi-directional charging for EVs, which can provide additional economic incentives for EV owners (Alexander, Crisostomo, Krell, Lu, & Ramesh, 2021; Coignard, Saxena, Greenblatt, & Wang, 2018), and aide in ensuring grid resilience, by enabling peak shaving and load shifting which will become increasingly important with the adoption of ever more variable renewable energy sources, as is projected to occur across North America (Murphy, et al., 2021; Williams, et al., 2020; BloombergNEF, 2021; Sepulveda, Jenkins, Sisternes, & Lester, 2018).

Ensuring adequate charging infrastructure will be particularly important as recent studies have found that it is feasible for heavy-duty trucking to increase its use of EVs with 80% of routes comprising 50% of fuel use are for trips shorter than 200 miles, availing the opportunity for depot charging to meet the needs of an electrified heavy-duty trucking sector (National Renewable Energy Lab, 2021). As the passenger vehicle and heavy-duty truck freight sectors in Canada account for 21% of total emissions (Environment and Climate Change Canada, 2021), widespread adoption of EVs for both passenger and heavy-duty transport could aide in significantly reducing emissions (Doluweera, Hahn, Bergerson, & Pruckner, 2020) (Knobloch, et al., 2020), particularly within urban areas (Sisson, 2021), providing for added cost savings through decreased health care costs (Health Canada, 2021).

Table 1 – Transport Emissions (Canada)

<table>
<tr><th>Emissions Source</th><th>Mt CO2 eq</th><th colspan="4">Percentage (%) of Total</th></tr>
<tr><td>Canada's Total Emissions (2019)</td><td>730</td><td>100.00%</td><td></td><td></td><td rowspan="5">21.02%</td></tr>
<tr><td>Canadian Transport Emissions Total (2019)</td><td>185.8</td><td>25.45%</td><td></td><td rowspan="4">82.59%</td></tr>
<tr><td>Freight - Heavy Duty Trucks</td><td>64.77</td><td>34.86%</td><td></td></tr>
<tr><td>Passenger Cars</td><td>33.63</td><td>18.10%</td><td rowspan="2">47.73%</td></tr>
<tr><td>Passenger - Light Trucks</td><td>55.06</td><td>29.63%</td></tr>
</table>

(Note: Environment and Climate Change Canada, 2021)

To meet the increased demand required to facilitate higher variable renewable energy penetration, several different energy storage systems have been developed. While battery technologies have made impressive advances in recent years, having tripled in energy density while experiencing precipitous cost declines over the past decade, they are still not able to provide long-term energy storage capabilities required for an increasingly renewable-integrated grid, requiring a 17-fold increase in deployed battery storage to meet a doubling in renewable energy capacity (IRENA, 2020, p. 41). Though lithium-ion batteries have become the preferred storage medium for transportation purposes, there are safety concerns with their use in stationary storage applications as such systems also pose a significant fire risk in the case of thermal runaway of the lithium cells (Duffy, 2021; Australian Associated Press, 2021). There are also challenges related to the manner in which the materials required for the manufacture of lithium-ion cells are derived (International Energy Agency, 2021; Schlossberg, 2021; Stratmann, Soetaert, Kersken, & Oevelen, 2021), as well as end-of-life considerations that could prove to be challenging to overcome given the number and scale of battery cells soon to require recycling, refurbishment or re-use, though efforts are being made to pro-actively address these challenges (Kelleher Environmental, 2019; U.S. Department of Energy, 2021; Willuhn, 2021; Lei, et al., 2021; Thompson, et al., 2020).

Pumped storage hydro is the main method of longer-duration energy storage, comprising 96% of the world's current storage capacity (IRENA, 2020, p. 41).
However, such systems are dependent on availability of particular conditions including suitable terrain and water availability and require large land areas (Sepulveda, Jenkins, Sisternes, & Lester, 2018).

Figure 3 – Pumped Storage Hydro & Lithium-Ion Battery System

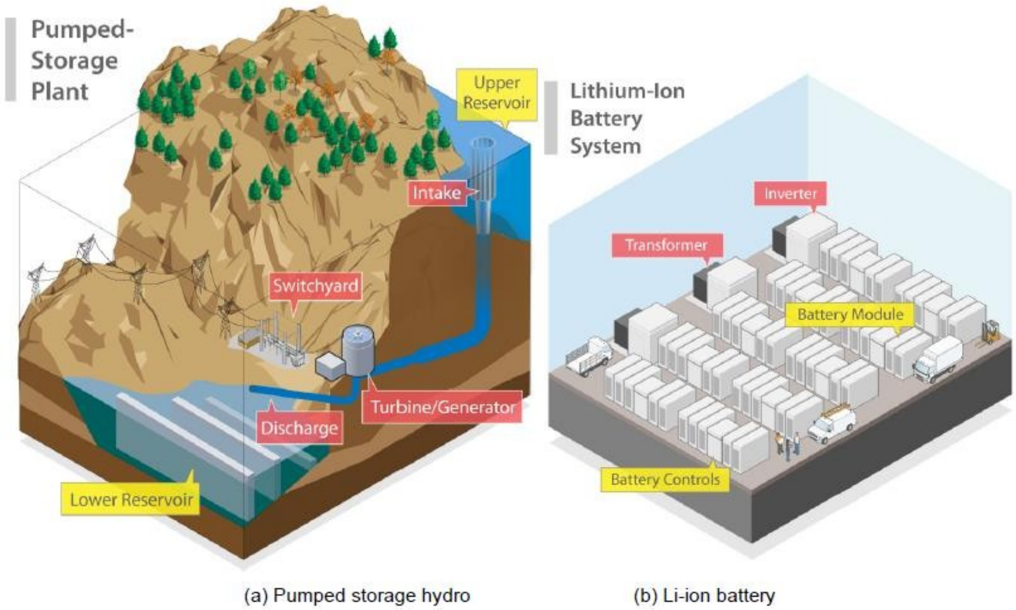

(Note: Denholm, Cole, Frazier, Podkaminer, & Blair, 2021)

Additional storage systems currently under development include redox-flow battery systems such as those designed by Primus Power (Primus Power, 2021), flywheel storage (OXTO Energy, 2021), gravity-fed energy storage systems (Energy Vault, Inc., 2021) (Ares North America, 2021), compressed air storage (Hydrostor, 2020), liquid air energy storage (Highview Power, 2021), and thermo-photovoltaic systems (Antora Energy, 2020). However, there are limitations of each of these systems as each is either location dependent, higher cost, shorter duration, requires greater land use, requires rare earth elements, has difficulties in scaling or is not yet commercially proven.

Other technologies, including thermal energy storage, are expected to fulfill the need of storing power for durations in excess of 8 hours (Denholm, Cole, Frazier, Podkaminer, & Blair, 2021). With a potential capacity of 100 GW of storage in the US market, longer-duration storage can provide additional benefits of enhancing the ability to match diurnal fluctuations in VRE output, enabling time-shifting and deferring the need for additional transmission capacity

(Denholm, Cole, Frazier, Podkaminer, & Blair, 2021). Coupling VRE resources, particularly solar, with longer-duration storage could enable VRE to provide more than half of all power produced on an annual basis (Denholm, Cole, Frazier, Podkaminer, & Blair, 2021).

Thermal energy storage does not experience the same losses in the storage-recovery cycle as either electrochemical or mechanical storage systems, returning nearly 99% of the initial energy input in the system (Sugo, Kisi, & Cuskelly, 2013). They also do not suffer from the effects of degradation attributed to electrochemical storage. Combined, these features make thermal energy storage ideal for longer-duration and high-cycle storage systems such as those required for EV charging applications.

To achieve the desired emissions reductions from the mass adoption of EVs, it will be important to consider the source of power for such systems. Solar powered thermal energy storage has been shown to be a viable technology in the local context, with the successful integration of solar thermal heating and underground thermal energy system deployed in the Drake Landing project in Okotoks, Alberta (IRENA, 2020, p. 94; Sudeyko & Greacen, 2017). Conversely, previous studies conducted within Alberta have indicated that efforts to meet the demand for EV charging utilizing on-site energy generation from solar photovoltaic energy is not feasible for generating the required amount of energy to meet charging demand for the expected influx of electric vehicles, and would require additional on-site storage capacity, or energy drawn from the grid to provide the necessary power for EV charging (Lefebvre, 2018). The increased energy density and efficiency afforded by concentrated solar power generation, coupled with the efficiency of the miscibility gap alloys (MGAs) used in the thermal energy storage seek to overcome this limitation.

The advantage of the CSP system selected for this study is that it provides for greater energy density using solar thermal collectors than solar photovoltaic panels, improving overall system efficiency (Smil, 2010) and also requires significantly less land area than existing CSP systems due to its compact, modular design (Kisi, et al., 2018; Reed, Sugo, & Kisi, 2018).

2.1 Miscibility Gap Alloys (MGAs)

Miscibility gap alloys are a type of binary metallic phase change material (PCM) that are used for thermal energy storage. Modular blocks composed of two thermodynamically stable, immiscible metals which contain "discrete, fully encapsulated, particles of a lower melting point metal trapped within a dense matrix of a higher melting point metal" (Kisi, et al., 2018, p. 2) operate under a narrow temperature range (±50°C, heat) (Kisi, et al., 2018; Reed, Sugo, & Kisi, 2018) to store energy as a combination of the "latent heat of fusion of the lower melting point metal and 100°C of sensible heat storage" (Kisi, et al., 2018, p. 2). The narrow temperature range of the latent heat of the miscibility gap alloys enables precise control of system parameters (Kisi, et al., 2018; Reed, Sugo, & Kisi, 2018).

Figure 4 – Miscibility Gap Alloys – Modular Blocks

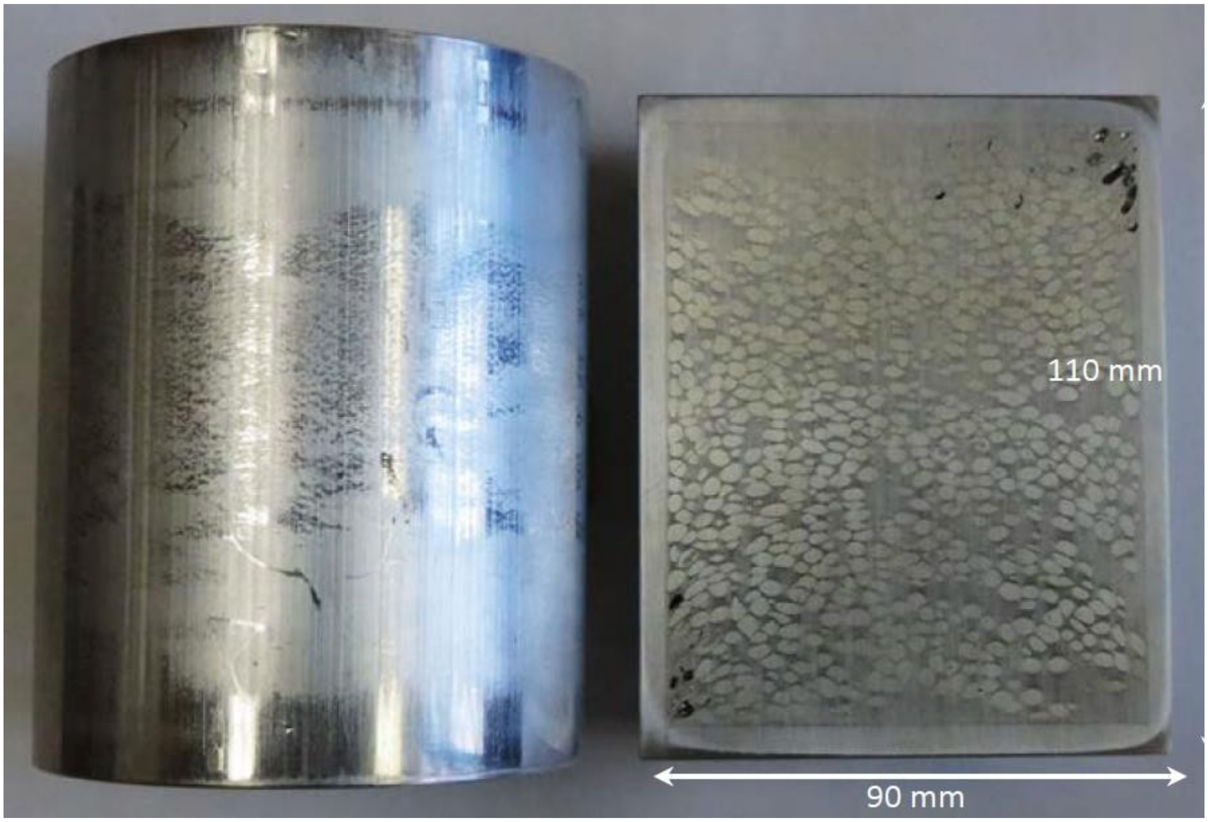

(Note: Kisi, et al., 2018)

Figure 5 – Miscibility Gap Alloys – Inverted Microstructure

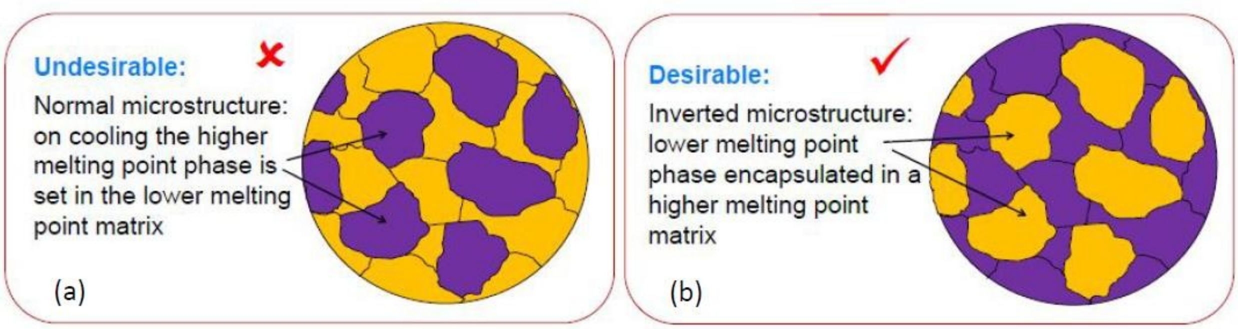

(Note: Kisi, et al., 2018)

MGAs provide benefits over existing phase change materials as they have high thermal conductivity (50 – 200 times greater than the majority of installed thermal storage materials) and high energy density and employ conductive rather than convective heating, which enables rapid, uniform heat distribution, and allows for greater energy storage in smaller volumes, thus reducing plant footprint and associated system costs (Kisi, et al., 2018; Reed, Sugo, & Kisi, 2018). Miscibility gap alloys exhibit decreased time delay between discharge-recharge cycles than other phase-change materials owing to the higher energy storage density per unit volume, and greater thermal conductivity of the miscibility gap alloys (Sugo, Kisi, & Cuskelly, 2013). As a result, the application of miscibility gap alloys combined with concentrated solar power generation is expected to provide significant cost and greenhouse gas emissions reductions potential, providing opportunities for load shifting and the ability to address intermittency concerns related to the diurnal nature of solar availability, and issues related to inclement weather (Sugo, Kisi, & Cuskelly, 2013).

Table 2 – Miscibility Gap Alloys – Phase Change Material Comparison

Candidate thermal storage systems compared with state of the art PCM (rows 1,2).

System	Fusible phase					Thermal conductivity of matrix (W/m K)
	Phase name	Melting point (°C)	Heat of fusion (kJ/kg)	Energy density (MJ/L)	Equivalent temperature range of sensible heat	
PCM-1 organic	Paraffin $C_{20\text{-}33}$ [5]	50	189	0.17	76	<1
PCM-2 salt	KNO_3–$NaNO_3$ eutectic [9]	221	100	0.204	70	<1
Al–Sn	Sn	232	59	0.43	257	237
Al–Bi	Bi	271	52	0.51	433	237
Fe–Mg	Mg	650	346	0.60	590	80
Fe–Cu	Cu	1085	205	1.84	526	80
SiC–Si	Si	1414	1926	4.49	2713	200

(Note: Sugo, Kisi, & Cuskelly, 2013)

Table 3 – Miscibility Gap Alloys – Thermal Properties

Calculated thermal properties of candidate MGA thermal storage media for $\Delta T = 100\,^{\circ}C$.

System	Phase change (°C)	Heat of fusion (kJ/L)	Energy density[a] (MJ/L)	Thermal conductivity[b] (W/mK)
C-Zn	420	843	0.62	100
C-Al	660	1071	0.9	158
C-(Al-Si)	577	1516	1.1	158
Molten salt[c]	N/A	N/A	0.27	< 0.7

[a] Energy density here includes $\pm$ 50 °C of sensible heat around the phase change temperature and ΔT of 100 °C for the molten salt.
[b] Thermal conductivity was calculated using the Lattice Monte Carlo technique (Rawson et al.).
[c] Sodium Nitrate (60%) and Potassium Nitrate (40%), ($NaNO_3 - KNO_3$).

(Note: Reed, Sugo, & Kisi, 2018)

As the material remains and behaves as a solid, the storage unit can be composed of modular blocks. The modular, scalable nature of the blocks enables opportunities for re-use and recycle; the blocks can be re-configured for new or different applications and, as MGAs are composed of immiscible metals, they can be readily separated by melting and recycled at end of life, further enhancing the economics of such systems through materials recovery at end-of-life with approximately 25% of material costs realized through salvage (Kisi, et al., 2018).

MGAs are versatile and adaptable and operate across a broad range of temperatures (232℃ Al-Sn to 1414℃ SiC-Si), making them suitable for a many different applications, including space heating, industrial processes, waste heat recovery and concentrated solar thermal energy generation, and energy storage (Sugo, Kisi, & Cuskelly, 2013).

Table 4 – Miscibility Gap Alloys - Thermal Properties Comparison

Type	Melting temperature of active phase (ºC)	Thermal conductivity (W/mK)	Energy density (MJ/L)*
Sn 50%- Al	230	120	0.43
Zn 50%- C	420	70	0.65
Mg 50%- Fe	650	100	0.58
Cu 50% - Fe	1085	200	1.2
Si 50% - SiC	1410	75	2.5

* All values include 100ºC of sensible heat capacity
‡ A convenient graphical method of displaying the thermal properties of MGA was pioneered in earlier work and may be consulted for further comparison with other storage materials (Rawson A., et al., 2014).

(Note: Kisi, et al., 2018)

As "more than 65% of the globally produced energy is lost as waste heat" (Zhou, et al., 2021, p. 1), with the annual thermal energy storage demand on the order of 10^{18}J in the US market alone, MGAs could provide for a low-cost form of thermal energy storage with the capability of reducing the use of fossil fuel generated energy, producing commensurate emissions reductions and environmental benefits (Sugo, Kisi, & Cuskelly, 2013). Lower conversion losses for thermal energy storage systems provide for more efficient storage than thermochemical, chemical and mechanical storage means, suffering only from environmental losses, which can be on the order of a few percent per day (Sugo, Kisi, & Cuskelly, 2013).

2.2 Solar thermoelectricity via advanced latent heat storage (STEALS)

Solar thermoelectricity via advanced latent heat storage (STEALS) system integrates several technologies utilizing aspects of concentrated solar power (CSP), thermal energy storage (miscibility gap alloys) and a thermoelectric generator into a compact, modular, scalable form. The STEALS system is a novel, fully-integrated solar electricity-generating technology that includes the solar receiver, phase-change material (PCM) thermal storage (in the form of miscibility gap alloys (MGAs), heat pipes, thermal valve, thermoelectric generators, and heat rejection in a single module, providing cost-effective, dispatchable power at a variety of scales, ranging from 10kW to 20MW (Olsen, et al., 2016; Glatzmaier, et al., 2017; Rea, et al., 2018). The design of the system, as a solid-state device that incorporates latent heat thermal energy storage combined with a thermal valve, eliminates the need for piping, valves, and pumps associated with circulating heat-transfer fluid as part of conventional concentrated solar power system designs, thus reducing operation and maintenance costs while enabling the STEALS system to deliver near-constant power generation at times shifted from peak sunlight hours, to peak demand hours, providing dispatchable electricity on demand (Olsen, et al., 2016; Glatzmaier, et al., 2017). The solid-state design has the added benefit of making the system inherently modular and scalable, overcoming the challenges faced by traditional CSP steam turbine plants, which require large scale deployments (minimum $50MW_e$) to be economically viable (Olsen, et al., 2016; Glatzmaier, et al., 2017).

Figure 6 – STEALS System Diagram

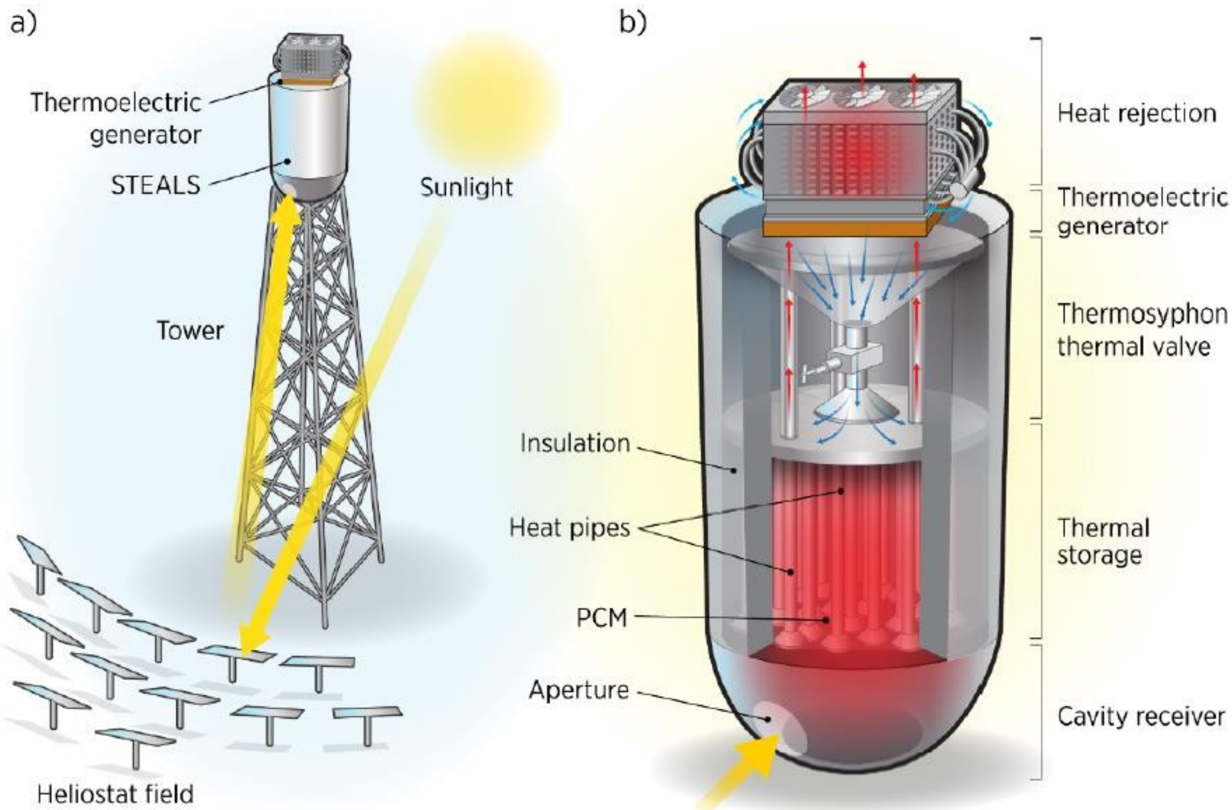

(Note: Rea, et al., 2018)

An array of heliostats (reflective mirrors) that use two-axis tracking reflect concentrated sunlight through an aperture in the bottom of the STEALS device, which is located atop a central tower. The concentrated sunlight is converted to heat via a solar absorber containing the phase-change material, which acts as both the solar receiver and thermal energy storage medium. The concentrated sunlight (1,000 kW/m^2) diverges at the point of the receiver, resulting in an average intensity of 100 kW/m^2 at the receiver surface (Olsen, et al., 2016). An absorption efficiency of 90% results in a heat flux density of 9W/cm^3 through the MGA (Olsen, et al., 2016). Thermal gradients within the STEALS device are minimized as heat pipes with extremely high thermal conductivity (10,000W/m/K) are embedded within the MGA, providing for a high thermal-conductivity pathway through the MGA (Olsen, et al., 2016; Rea, et al., 2018). The heat pipes work in tandem with a thermal valve (valved thermosyphon) controlling the rate at which the heat is then delivered to the thermoelectric generator (TEG) module where it is used either for direct electricity generation, or to charge the MGA for thermal energy storage, enabling subsequent generation during off-sun hours, or both for simultaneous electricity production and energy storage (Olsen, et al., 2016; Glatzmaier, et al., 2017; Rea, et al., 2018). The STEALS module has an operating temperature of 650°C and the heat valve is 90% efficient, resulting in less than a 50°C temperature drop between the MGA and hot side of the TEG when the system is operating, which is crucial as the thermoelectric generator is reliant upon a stable temperature range for optimum performance (Olsen, et al., 2016). The narrow operating range of the latent heat of the MGAs, provide a precise temperature range during system operation providing for ideal system design and compatibility of the two technologies (Kisi, et al., 2018). The TEGs have a projected thermal-to-electric energy conversion efficiency of 9 percent, and the output power of the system scales linearly with the size of the TEG array (Olsen, et al., 2016). Having no moving parts, these solid-sate devices have been shown to work for decades without the need for maintenance, reducing overall system cost (Olsen, et al., 2016).

Excess heat is vented through the top of the STEALS module through a finned, air-cooled heat exchanger (Glatzmaier, et al., 2017). The configuration of the system limits convective losses of the STEALS module at the receiver and allows for improved heat flow throughout the system by enabling gravity-assisted liquid return through the embedded heat pipes (Olsen, et al., 2016). By directly integrating the thermal energy storage and power block components together with the solar receiver, the STEALS system reduces the length of pathways for heat, thereby reducing thermal losses, making the system nearly isothermal with a combined receiver optical and thermal efficiency of 95 %, and reducing system cost compared to traditional concentrating solar power designs, thus enabling a modular system design that allows for dispatchable solar electricity generation at a lower levelized cost of energy (LCOE) than traditional CSP or solar PV plus battery systems (Olsen, et al., 2016; Glatzmaier, et al., 2017). Previous techno-economic analysis of a 100 kW system located in Daggett, CA showed favourable LCOE for STEALS systems when compared to a solar PV plus battery; 11.7- 11.9 cents/kWh versus 15-25 cents/kWh for solar plus battery (Glatzmaier, et al., 2017)

Microgrids have been identified as the best application for the STEALS system, with LCOE for STEALS systems relatively constant for systems ranging in size from 20 kWe to 1 MWe, with minimum LCOE achieved for systems sized at 100 kWe. The relatively constant LCOE for STEALS systems is due to the trade-off in optical efficiency resulting from reduced heliostat field size and cost, to improved storage efficiency as a result of improved surface area to volume ratio (Glatzmaier, et al., 2017).

Half of all current microgrids are for systems smaller than 1 MWe in size, considered to be the best market for future STEALS installations, and can be utilized for applications ranging from isolated communities and mines, to residential communities, commercial applications, public institutions (hospitals, universities, etc.) and military installations. Cost reduction and reliability are considered to be the main motivating factors for isolated installations, while community installations are motivated by desires for locally produced renewable sources of electricity (Glatzmaier, et al., 2017).

Locational factors, particularly solar resource availability, which is influenced by latitude, affects the efficiency of STEALS (Glatzmaier, et al., 2017). At higher latitudes, with greater seasonal variation in solar irradiance, larger heliostat fields and solar multiples are required to achieve high-capacity factors and maintain dispatchability of the system, requiring larger thermal storage systems that can reduce the feasibility of STEALS, adversely impacting the LCOE (Glatzmaier, et al., 2017). Simulations that attempt to control for labour and locational factors found that a STEALS system deployed in Soldotna, Alaska had twice the LCOE of a STEALS system deployed in Gila, Arizona, despite both locations having similar labour market factors, owing predominantly to the lower solar resource in Alaska (Rea, et al., 2018).

Figure 7 – STEALS System – Heliostat Array Based on Location

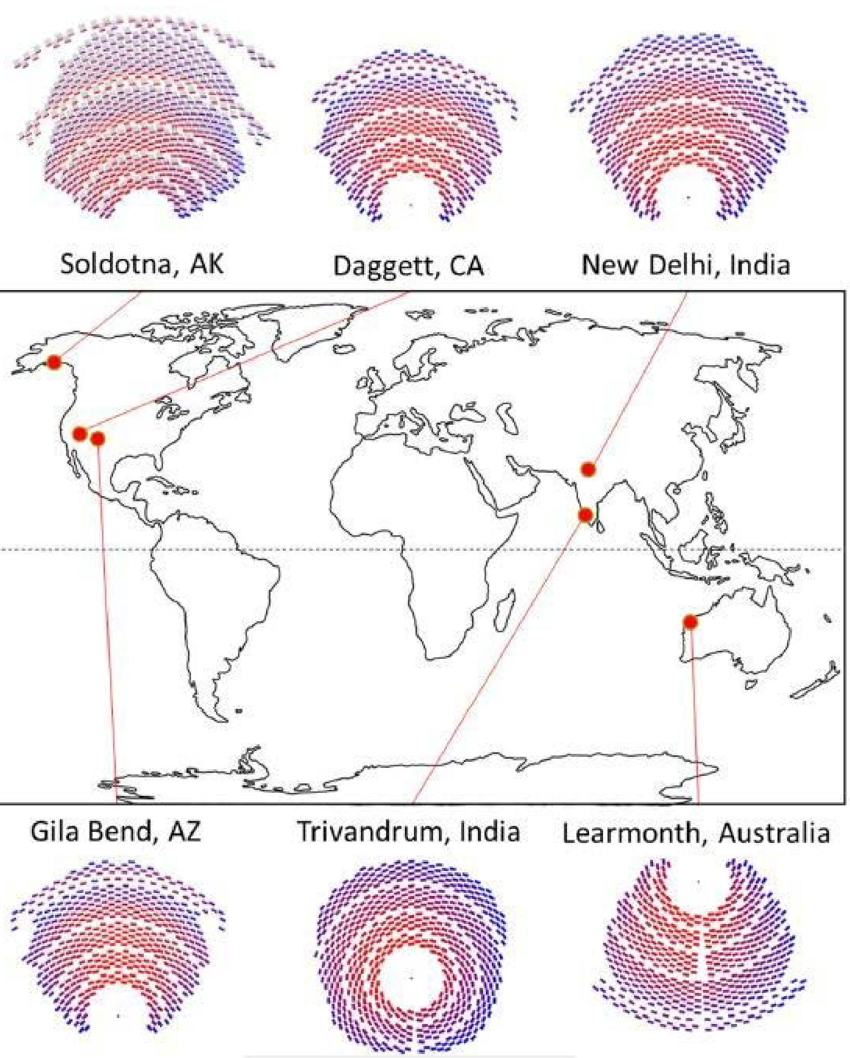

(Note: Rea, et al., 2018)

CHAPTER 3: METHODOLOGY

I will first outline the methodology that was used to estimate the number of electric vehicles that will visit the EV charging station each day, and annually. I will then discuss the methodology that was used to calculate the energy, environment, and economic dimensions of my analysis.

3.1 Number of Vehicles Using the Charging Station

First, I needed to determine the number of vehicles that would be charged each day, and throughout the year. In my calculations, an estimate of three vehicles charged per hour was used. An assumption of a 100% utilization rate was used over the span of 15-hour daily operations throughout the duration of the year (See Appendix A – Energy Calculations).

3.2 Determination of the Energy Requirements for EV Charging

To start, I determined the energy demand of a Tesla Model 3 battery pack (Lambert, 2020) which was used as a proxy estimate of the average battery pack size of vehicles that would make use of the EV charger. I then estimated the depth of discharge of the average EV battery pack requiring charging and multiplied that by the estimated average turnover or throughput of the charging infrastructure based on the anticipated utilization rate of 100% to determine the number of vehicles charged per hour to determine hourly charging requirements. I multiplied this number by an estimated 15-hours of daily operations to determine daily energy requirements. This value was then multiplied by 365 days to determine annual energy requirements for EV charging (See Appendix A – Energy Calculations).

To determine system component sizing, requirements of 6 hours of daytime charging and 9 hours of storage, based on average hourly energy demand, were used for each of the respective system designs; solar PV + battery storage & solar PV plus STEALS storage.

Efficiency losses of 15%, an approximation for the average 85% efficiency of battery storage systems (Doluweera, 2021), were calculated for the battery component of the solar PV + battery storage system to ensure that the solar PV array was adequately sized to provide enough power to meet energy demands. Once system component sizes had been determined, SAM was used to provide a model of the solar PV plus battery system. Climactic data was downloaded from Natural Resources Canada for use in the SAM model for the given location of Medicine Hat, Alberta (Natural Resouces Canada, 2020). In the SAM modelling software, a system design with a nameplate capacity of 810 kWdc with a DC to AC ratio of 1.2 and an inverter efficiency of 96% was used. The system model employed an array with 1-axis tracking, 0 tilt degrees and a 180° azimuth, generating a system with total losses of 12.6% (See Appendix A – Energy Calculations).

A literature review was undertaken to determine the capacity factor based on solar irradiance of location for the STEALS system for Daggett, California (Glatzmaier, et al., 2017). Information for solar irradiance and capacity factor for solar PV installations was then derived from the PVWatts website for the location of Daggett, California and Medicine Hat, Alberta, respectively (National Renewable Energy Laboratories, n.d.). The information derived from PVWatts, also included a system design using 1-axis tracking (See Appendix E – PVWatts Solar Irradiance, Capacity Factor) to increase solar irradiance and capacity factors, providing for equivalent system design parameters to that used to model the solar PV plus battery storage system in SAM (See Appendix A – Energy Calculations). The solar irradiance and capacity factor information derived for Medicine Hat, Alberta through PVWatts was used to determine the equivalent capacity factor for the STEALS system for Medicine Hat, Alberta. This information was then used to determine the sizing of the system components for the solar PV plus STEALS storage system.

Again, SAM was used to model the solar PV component of the solar PV plus STEALS system. Climactic data was downloaded from Natural Resources Canada for use in the SAM model for the given location of Medicine Hat, Alberta (Natural Resouces Canada, 2020). In the SAM modelling software, a system design with a nameplate capacity of 300 kWdc with a DC to AC ratio of 1.2 and an inverter efficiency of 96% was used. The system model employed an array with 1-axis tracking, 0 tilt degrees and a 180° azimuth, generating a system with total losses of 12.6% (See Appendix A – Energy Calculations).

3.3 Determination of Emissions Reductions

To determine the amount of CO_{2e} emissions reductions from using renewable energy generation for EV charging, a calculation of the total annual energy requirements for the system, and the electricity grid displacement factor with renewable generation for the Alberta grid (Government of Alberta, 2019) were used. The total annual energy requirements, previously calculated as kWh/yr were converted to MWh/yr and the electricity grid displacement factor for renewable generation (Government of Alberta, 2019) was then applied to determine total annual emissions reduction as a result of using renewable generation for EV charging.

3.4 Determination of Economic factors (LCOE) for Respective Systems

As part of the system simulation using SAM modeling software, a LCOE was generated for the solar PV plus batter system.

Similarly, as part of the system simulation using SAM modeling software, a LCOE was generated for the solar PV component of the solar PV plus STEALS system.

A literature review was undertaken to determine the LCOE of the STEALS system for the location of Daggett, California (Glatzmaier, et al., 2017). The LCOE value of the STEALS system for Daggett, California was multiplied by the high-level capacity factor of the STEALS system for Daggett, California (Glatzmaier, et al., 2017) and divided by the proxy high-level capacity factor for Medicine Hat (derived from the process described previously) to determine a proxy LCOE for Medicine Hat.

A weighted-average LCOE for the total solar PV plus STEALS system was determined by multiplying the hourly energy requirements for the requisite number of hours of daytime charging by the LCOE determined for the solar PV component of the solar PV plus STEALS system (as derived by SAM modeling). This value was then added to a calculation of the hourly energy requirements the requisite number of daily storage hours multiplied by the proxy LCOE of the STEALS component for Medicine Hat, which was divided by 100 to provide a weighted-average LCOE for the solar PV plus STEALS system design (See Appendix C – Economic Calculations).

CHAPTER 4: RESULTS & DISCUSSION

Listed below is a flow diagram outlining the process for determining the values, inputs and system modelling included as part of the calculations for the energy, environmental and economic components of my analysis. All subsequent calculations are derived from the initial starting point of determining EV charging system requirements. The calculations are discussed in greater detail, below.

Figure 8 – Analysis Process Flow Diagram

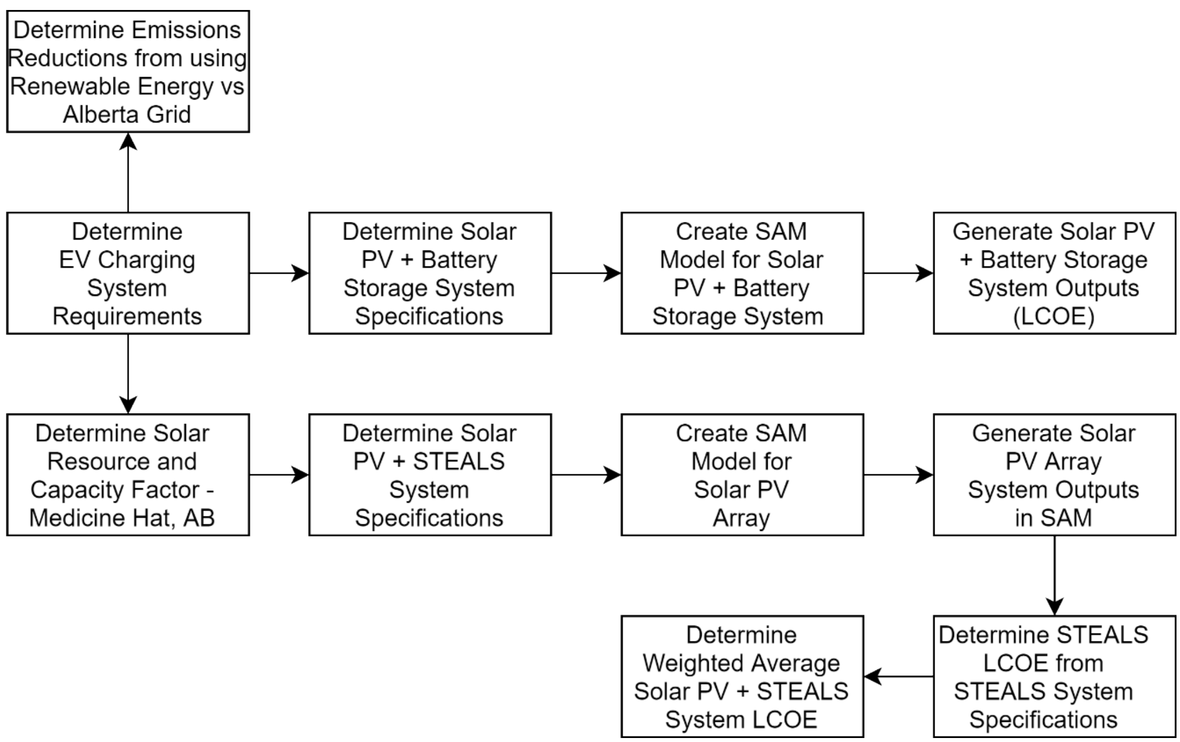

(Note: Choveaux, 2021)

4.1 Number of vehicles visiting a charging station each day

For this calculation, I assumed the site would be able to accommodate 3 EVs charging per hour, over a daily operating duration of 15 hours, operating 365 days a year, for an estimated throughput of 16,425 total vehicles charged annually.

Table 5 - EV Charging System - Vehicle Throughput

EV Charging System - Vehicle Throughput		
Number of vehicles per hour	3	vehicles per hour
Daily Hours of Operation	15	Hours
Days per Year	365	Days
Total Vehicles Charged	16,425	Annually

(Note: Choveaux, 2021)

4.2 Energy Calculations

The Tesla Model 3 battery pack, with an 82 kWh capacity (Lambert, 2020), was used as a proxy for the average battery pack size in energy calculations. Each vehicle was estimated to have a depth of discharge of 80% of the battery pack. Charging 3 vehicles per hour would require a total energy requirement of 196.8 kWh per hour. With daily operations of 15 hours, total daily energy requirements were calculated as 2,952 kWh/day. Over the span of 365 days, total annual energy requirement was determined to be 1,077,480 kWh/yr.

Table 6 – EV Charging System Requirements

EV Charging System Requirements		
Number of vehicles per hour	3	vehicles per hour
Size of battery pack	82	kWh
Depth of Discharge	80	%
Hourly Energy Demand	196.8	kWh
Daily Hours of Operation	15	hours
Daily Energy Requirements	2952	kWh
Yearly Energy Requirements	1,077,480	kWh/yr

(Note: Choveaux, 2021)

The EV charging system is designed to mostly function independently, but limitations due to seasonality of solar irradiance require the system to still be connected to the grid. Over the 15 hours of daily operation, the system was modeled to provide 6 hours of daytime charging, requiring 9 hours of storage capacity for both battery and STEALS storage systems. Daytime charging was calculated as 6 hours of operation multiplied by the hourly energy demand of 196.8 kWh, resulting in a solar PV array sizing of 1,181 kWh for daytime charging. The total capacity for the battery was calculated as 9 hours multiplied by the hourly energy demand of 196.8 kWh, resulting in a minimum battery capacity of 1,771 kWh. An adjustment must be made based on the overall efficiency of the battery pack, estimated as 85% efficient, to ensure adequate charging of the system, requiring a solar PV array of 2,084 kWh for battery charging, resulting in overall daily energy requirements of 3,265 kWh, including system losses.

Table 7 – Solar PV + Battery Storage System Specifications

Solar PV + Battery Storage System Specifications		
Daily Energy Requirements (including system losses)	3,265	kWh
Solar PV Array - Daytime Charging	1,181	kWh
Solar PV Array (Battery Charging)	2,084	kWh
Battery Size (9 hour storage)	1,771	kWh

(Note: Choveaux, 2021)

To determine system sizing requirements for the solar PV + STEALS system, a literature review was undertaken to determine comparable capacity factors for the given location of Medicine Hat, Alberta. Previous studies had provided information on capacity factors for the STEALS system for the location of Daggett, California (Glatzmaier, et al., 2017). Using PV Watts, Daggett, CA was found to have a direct nominal solar irradiance of 7.90 kWh/m^2/day, producing a capacity factor of 25.2 for solar PV installations (National Renewable Energy Laboratories, n.d.). Given that the literature provided a higher capacity factor for the STEALS system on the order of 31.4-38.1 (Glatzmaier, et al., 2017), this information was then used to make a proxy estimate of the potential capacity factor for the STEALS system when located in Medicine Hat, Alberta.

Again, PVWatts was used to determine the direct nominal irradiance for Medicine Hat, Alberta of 4.91 kWh/m^2/day, with a capacity factor of 16.4 for a solar PV array (National Renewable Energy Laboratories, n.d.). Given these factors, it was determined that a STEALS system located in Medicine Hat, Alberta would provide a capacity factor ranging from 19.5 to 23.7.

Table 8 - Solar Resource and Capacity Factor - Medicine Hat, AB

Solar Resource and Capacity Factor - Medicine Hat, AB		
Solar PV	Daggett, CA	Medicine Hat, AB
Direct Nominal Irradiance	7.90kWh/m^2/day	4.91kWh/m^2/day
Capacity Factor	25.2	16.4
STEALS	Daggett, CA	Medicine Hat, AB
Direct Nominal Irradiance	7.90kWh/m^2/day	4.91kWh/m^2/day
Capacity Factor (Low)	31.4	19.5
Capacity Factor (High)	38.1	23.7

(Note: Choveaux, 2021)

To compare the systems, I used the US National Renewable Energy Laboratories System Advisor Model to model the solar PV plus battery energy storage system. I uploaded location and resource data for Medicine Hat, Alberta (Natural Resources Canada, n.d.) into the SAM modeling software. In the SAM modelling software, a system design with a nameplate capacity of 810 kWdc with a DC to AC ratio of 1.2 and an inverter efficiency of 96% was used. The system model employed an array with 1-axis tracking, 0 tilt degrees and a 180° azimuth, generating a system with total losses of 12.6% (See Appendix A – Energy Calculations).

The solar PV component of the solar PV plus STEALS system was modelled using the SAM software. Given the difference in capacity factors for the different storage mediums, it was determined that a solar PV system plus STEALS would require a 300 kW solar PV array. This solar array would then be couple with a 450 kW STEALS storage system to produce requisite energy demand for EV charging.

4.3 Environmental Calculations

To determine the amount of CO_{2e} emissions reductions from using renewable energy generation for EV charging, I looked at the total annual energy requirements for the system, 1,077,480 kWh/yr and the electricity grid displacement factor with renewable generation for the Alberta grid. I converted the total annual energy requirements to MWh/yr and then applied the electricity grid displacement factor for renewable generation of 0.53tCO_{2e}/MWh (Government of Alberta, 2019), to determine a total annual emissions reduction of 571.06 tCO_{2e}/year displaced as a result of using renewable generation for EV charging.

Figure 9 – Electricity Grid Displacement Factors (Alberta)

Factor	t CO_2e/MWh	Description
Electricity grid displacement factor		
Electricity grid displacement with renewable generation	0.53	Applicable to projects displacing grid–electricity with renewable generation.
Electricity grid displacement factor with line loss applied		
Increased on-site grid electricity use (includes line loss)	0.57	Applicable for use in projects that increase electricity usage in the project condition.
Reduction in grid electricity usage (includes line loss)	0.57	Applicable to energy efficiency projects resulting in decreased grid electricity usage in the project condition.
Distributed renewable displacement at point of use (includes line loss)	0.57	Applicable to projects displacing grid electricity with distributed renewable electricity generation at point of use.

2018 Electricity Grid Displacement Discussion Paper, calculation methodology is based on 2007 EDC Associates, Calculation of the Grid Emission Intensity Factor for Alberta.

(Note: Government of Alberta, 2019)

Table 9 - EV Charging System Requirements & Emissions Reductions

EV Charging System Requirements & Emissions Reductions		
Yearly Energy Requirements	1,077.48	MWh/year
Electricity Grid Displacement Factor	0.53	tCO_{2e}/MWh
Annual Emissions Reductions	571.06	Total tCO_{2e}/year

(Note: Choveaux, 2021)

4.4 Economic Calculations

The total capacity for the battery was calculated as 9 hours multiplied by the hourly energy demand of 196.8 kWh, resulting in a minimum battery capacity of 1,771 kWh. Using an average cost estimate of $250/kWh installed, total battery costs determined to be $442,800. Assuming a battery replacement would be required after 10 years operations, LCOE for the solar PV plus battery energy storage system increased from 17.48 cents/kWh to 18.77 cents/kWh with the battery replacement factored in.

Table 10 - Solar PV + Battery Storage System Specifications

Solar PV + Battery Storage System Specifications		
Daily Energy Requirements (incl system losses)	3265	kWh
Solar PV Array - Daytime Charging	1181	kWh
Solar PV Array (Battery Charging)	2084	kWh
Battery Size (9 hour storage)	1771	kWh
LCOE PV + Battery (no battery replacement)	17.48	cents/kWh
LCOE PV + battery (battery replacement year 10)	**18.77**	cents/kWh

(Note: Choveaux, 2021)

The 300 kW solar PV array modeled in SAM had a LCOE of 14.67 cents/kWh. A literature review found that the high-end LCOE for a STEALS system to be 11.9 cents/kWh. Utilizing the high-end capacity factor of 23.7 for the Medicine Hat location, the STEALS component of the system had a LCOE of 19.13 cents/kWh, producing a total weighted average LCOE for the solar PV plus STEALS system design of 17.35 cents/kWh, producing a lower LCOE than the solar PV plus battery system.

Table 11 - Solar PV + STEALS Storage System Specifications

Solar PV + STEALS Storage System Specifications		
Solar PV Array	300	kW
STEALS system (9hr storage)	450	kW
LCOE PV	14.67	cents/kWh
LCOE STEALS	19.13	cents/kWh
Wgt Avg LCOE PV + STEALS	**17.35**	cents/kWh

(Note: Choveaux, 2021)

CHAPTER 5: CONCLUSION & FUTURE WORK

The viability of the STEALS system has been shown to be effective in a northerly latitude, given that the location selected has abundant solar irradiance, as is the case for Medicine Hat, AB.

A comparative techno-economic analysis of solar PV plus battery storage and solar PV plus STEALS utilizing MGAs as the thermal energy storage medium determined that thermal energy storage is a viable storage medium to pair with solar photovoltaic systems, providing for a lower overall LCOE. Given the enhanced economics of the solar PV + STEALS system design over the solar PV + battery energy storage system, it is recommended that options for STEALS deployment in other applications be pursued, including for community microgrid and mining applications, industrial processes, and for space heating.

5.1 Limitations

Both MGAs and STEALS are early-stage technologies and will require continued development and advancement towards commercialization to be viewed as truly viable technologies. As the technologies are based on theoretical models or small-scale deployments, continued research and development for both MGAs and STEALS could lead to further cost reductions and improved performance. Preliminary testing suggests that STEALS system components, namely the thermosyphon valve will work more efficiently at larger scales (Rea, et al., 2018).

This research did not include an assessment of the additional emissions reductions that are expected to result from the transition from internal combustion engine vehicles to electric vehicles, producing potentially considerable additional environmental benefits.

5.2 Future Research

To date, a complete LCA has not been conducted for MGAs (Kisi, 2021). A determination of the emissions related to production of different materials and production processes would aid in determining overall emissions reductions potential throughout the product lifecycle. MGAs use abundant, recycled and recyclable materials, and are able to be repurposed and reconfigured to optimize system design for different use cases and applications, extending product lifecycle and enhancing sustainability metrics (Kisi, et al., 2018). The availability, recyclability, and ease with which the constituent materials can be recycled should provide for a favourable LCA over competing storage mediums, particularly batteries. Additional recent advancements in the production process for high temperature alloy materials (SiC) could lead to further emissions reductions in the manufacturing process and enhanced LCA metrics by utilizing plant-based material inputs that will provide some carbon sequestration benefits as part of the material inputs (Salk Institute, 2021; Thomas, Shin, Clair, & Noel, 2021).

Improvements in system component functionality, particularly in the form of higher efficiency thermoelectric generators (TEG) could also increase emissions reductions and reduce overall system costs of the STEALS system through enhanced performance and reduction in the need for additional system components, namely a smaller heliostat array (Zhou, et al., 2021; Glatzmaier, et al., 2017).

Site-specific EIAs would need to be undertaken for each of the systems studied, with particular attention paid to land use considerations of the STEALS system when compared to solar PV installations and traditional CSP system designs. Potential wildlife impacts related to the use of heliostat arrays as part of the STEALS system would also need to be assessed and any potential issues addressed.

A determination of additional/best use case for thermal energy storage, particularly miscibility gap alloys should be undertaken to determine impact of expected future cost reductions on the economics of each system.

Considerations for additional cost reductions in both solar PV cells and battery technology as the technologies mature and production scales up, providing for more rapid descent of learning curves and continued decline of system costs.

An LCA to evaluate the potential for enhanced system economics and environmental benefits of incorporating recycled content in both battery and solar PV cell design and manufacture.

REFERENCES

Alberta Electric System Operator. (2021). *AESO 2021 Long-Term Outlook.* Calgary, AB: Alberta Electric System Operator. Retrieved from https://www.aeso.ca/assets/Uploads/grid/lto/2021-Long-term-Outlook.pdf

Alexander, M., Crisostomo, N., Krell, W., Lu, J., & Ramesh, R. (2021). *Assembly Bill 2127 Electric Vehicle Charging Infrastructure Assessment: Analyzing Charging Needs to Support Zero-Emission Vehicles in 2030 – Commission Report.* California Energy Commission. Retrieved from https://www.energy.ca.gov/publications/2020/assembly-bill-2127-electric-vehicle-charging-infrastructure-assessment-analyzing

Antora Energy. (2020). *Home | Antora Energy*. Retrieved from Antora Energy: https://www.antoraenergy.com/home-1

Ares North America. (2021). *Ares North America - Gravity Line*. Retrieved from Ares North America: https://aresnorthamerica.com/gravityline/

Australian Associated Press. (2021, August 2). *Tesla big battery fire in Victoria under control after burning more than three days*. Retrieved from The Guardian: https://www.theguardian.com/australia-news/2021/aug/02/tesla-big-battery-fire-in-victoria-burns-into-day-three

BloombergNEF. (2021). *Sustainable Energy in America 2021 Factbook.* BloombergNEF. Retrieved from https://bcse.org/factbook/

Clean Energy Canada. (2021, May 19). *Canada has a once-in-generation opportunity to be a global battery leader if we act now: industry stakeholders*. Retrieved from Clean Energy Canada: https://cleanenergycanada.org/canada-has-a-once-in-generation-opportunity-to-be-a-global-battery-leader-if-we-act-now-industry-stakeholders/

Clean Energy Canada. (2021a, June 29). *Canada's updated 100% zero-emission vehicle sales target points to a clear solution*. Retrieved from Clean Energy Canada: https://cleanenergycanada.org/canadas-updated-100-zero-emission-vehicle-sales-target-points-to-a-clear-solution/

Coignard, J., Saxena, S., Greenblatt, J., & Wang, D. (2018). Clean vehicles as an enabler for a clean electricity grid. *Environmental Research Letters*, 1-8. doi:https://doi.org/10.1088/1748-9326/aabe97

Dao, C. (2021, August 17). *Officials forecast hundreds of thousands of electric vehicles in Alberta by 2041*. Retrieved from Global News: https://globalnews.ca/news/8120754/alberta-electric-vehicles-forecast/

Denholm, P., Cole, W., Frazier, A. W., Podkaminer, K., & Blair, N. (2021). *The Four Phases of Storage Deployment: A Framework for the Expanding Role of Storage in the US Power System.* Golden, CO: National Renewable Energy Laboratory. Retrieved from https://www.nrel.gov/docs/fy21osti/77480.pdf

Doluweera, G. (2020a, November). *SEDV Capstone Project Ideas_CERI_Presentation Final*. Retrieved January 21, 2021, from D2L - University of Calgary: https://d2l.ucalgary.ca/d2l/le/content/324307/viewContent/4352145/View

Doluweera, G. (2021, July 27). (I. Choveaux, Interviewer)

Doluweera, G., Hahn, F., Bergerson, J., & Pruckner, M. (2020). A scenario-based study on the impacts of electric vehicles on energy consumption and sustainability in Alberta. *Applied Energy*. doi:https://doi.org/10.1016/j.apenergy.2020.114961

Donaldson, A. (2019, April 23). *Finding a place to charge your EV is easy with Google Maps*. Retrieved from Google - Product Updates: https://www.blog.google/products/maps/finding-place-charge-your-ev-easy-google-maps/

Duffy, K. (2021, August 2). *A giant Tesla battery pack burst into flames during testing, and it took 150 firefighters 4 days to put out*. Retrieved from Business Insider: https://www.businessinsider.com/tesla-megapack-battery-fire-burns-four-days-testing-australia-2021-8

Edelstein, S. (2021, February 7). *Because of EV adoption, Norway nearly leads the world in per-capita electricity use*. Retrieved from Green Car Reports: https://www.greencarreports.com/news/1131201_because-of-ev-adoption-norway-nearly-leads-the-world-in-per-capita-electricity-use

Energy Vault, Inc. (2021). *About Us - Energy Vault*. Retrieved from Energy Vault, Inc.: https://energyvault.com/

Environment and Climate Change Canada. (2021). *Canadian Environmental Sustainability Indicators: Greenhouse gas emissions.* Gatineau QC: Environment and Climate Change Canada. Retrieved from https://www.canada.ca/content/dam/eccc/documents/pdf/cesindicators/ghg-emissions/2021/greenhouse-gas-emissions-en.pdf

Evannex. (2021, January 30). *President Biden Wants To Roll Out 500K New EV Chargers: Is It Possible?* Retrieved from Inside EVs: https://insideevs.com/news/483154/president-biden-plan-ev-charging-infrastructure/

Glatzmaier, G. C., Rea, J., Olsen, M. L., Oshman, C., Hardin, C., Alleman, J., . . . Ginley, D. S. (2017). Solar thermoelectricity via advanced latent heat storage: A cost-effective small-scale CSP application. *AIP Conference Proceedings 1850 - SolarPACES 2016* (pp. 030019-1 - 030019-8). AIP Publishing. doi:https://doi.org/10.1063/1.4984362

Government of Alberta. (2019, November 18). *Carbon Offset Emission Factors Handbook 2.0.* Retrieved from Government of Alberta: https://open.alberta.ca/dataset/2a41f622-5ae4-4985-838f-497e6afd110c/resource/0ba7b3dc-0658-43dc-b977-4c9c35637f49/download/aep-carbon-offset-emissions-factors-handbook-v-2-2019-11.pdf

Government of Canada. (2021, April 15). *Greenhouse gas emissions*. Retrieved from Government of Canada: https://www.canada.ca/en/environment-climate-change/services/environmental-indicators/greenhouse-gas-emissions.html

Harto, C. (2020). *Electric Vehicle Ownership Costs: Chapter 2—Maintenance.* Consumer Reports. Retrieved from https://advocacy.consumerreports.org/wp-content/uploads/2020/09/Maintenance-Cost-White-Paper-9.24.20-1.pdf

Health Canada. (2021). *Health Impacts of Air Pollution in Canada: Estimates of Premature Deaths and Nonfatal Outcomes.* Ottawa, ON: Health Canada. Retrieved from https://www.canada.ca/content/dam/hc-sc/documents/services/publications/healthy-living/2021-health-effects-indoor-air-pollution/hia-report-eng.pdf

Henze, V. (2020, December 16). *Battery Pack Prices Cited Below $100/kWh for the First Time in 2020, While Market Average Sits at $137/kWh*. Retrieved from Bloomberg NEF: https://about.bnef.com/blog/battery-pack-prices-cited-below-100-kwh-for-the-first-time-in-2020-while-market-average-sits-at-137-kwh/

Highview Power. (2021). *Technology | Highview Power*. Retrieved from Highview Power: https://highviewpower.com/technology/

Hoover, Z., Nägele, F., Polymeneas, E., & Sah, S. (2021, January 5). *How charging in buildings can power up the electric-vehicle industry*. Retrieved from McKinsey & Company: https://www.mckinsey.com/industries/electric-power-and-natural-gas/our-insights/how-charging-in-buildings-can-power-up-the-electric-vehicle-industry#

Hydrostor. (2020). *Technology - Hydrostor*. Retrieved from Hydrostor: https://www.hydrostor.ca/technology/

International Energy Agency. (2021). *The Role of Critical Minerals in Clean Energy Transitions.* International Energy Agency. Retrieved from https://www.iea.org/reports/the-role-of-critical-minerals-in-clean-energy-transitions

IRENA. (2020). *Innovation Outlook: Thermal Energy Storage.* Abu Dhabi: International Renewable Energy Agency. Retrieved from https://www.irena.org/-/media/Files/IRENA/Agency/Publication/2020/Nov/IRENA_Innovation_Outlook_TES_2020.pdf

Kane, M. (2021, February 13). *Shell Plans To Deploy Around 500,000 Charging Points Globally By 2025*. Retrieved from Inside EVs: https://insideevs.com/news/487881/shell-plans-500000-charging-points-globally-2025/

Kelleher Environmental. (2019). *Research Study on Reuse and Recycling of Batteries Employed in Electric Vehicles: The Technical, Environmental, Economic, Energy and Cost Implications of Reusing and Recycling EV Batteries.* Energy API. Retrieved from https://www.api.org/~/media/Files/Oil-and-Natural-Gas/Fuels/Kelleher%20Final%20EV%20Battery%20Reuse%20and%20Recycling%20Report%20to%20API%2018Sept2019%20edits%2018Dec2019.pdf

Kisi, E. (2021, August 5). (I. Choveaux, Interviewer)

Kisi, E., Sugo, H., Cuskelly, D., Fiedler, T., Rawson, A., Post, A., . . . Reed, S. (2018). Miscibility Gap Alloys – A New Thermal Energy Storage Solution. *World Renewable Energy Congress XVI* (pp. 1-7). Murdoch: ResearchGate. doi:DOI: 10.1007/978-3-319-69844-1_48

Knobloch, F., Hanssen, S. V., Lam, A., Pollitt, H., Salas, P., Chewpreecha, U., . . . Mercure, J.-F. (2020, June). Net emission reductions from electric cars and heat pumps in 59 world regions over time. *Nature Sustainability*, 437-447. https://doi.org/10.1038/s41893- 020-0488-7

KPMG. (2021, 25 February). *Electric Vehicles to make up majority of new car purchases*. Retrieved from KPMG: https://home.kpmg/ca/en/home/media/press-releases/2021/02/electric-vehicles-to-make-up-majority-of-new-car-purchases.html

Lambert, F. (2020, November 10). *Tesla confirms new 82 kWh battery pack in Model 3, thanks to new cells*. Retrieved from Electrek: https://electrek.co/2020/11/10/tesla-model-3-82-kwh-battery-pack-new-cells/

Lefebvre, N. (2018). *A Comparison of Grid Power and Solar Power for Electric Vehicle Fast Charging*. University of Calgary. Retrieved from https://d2l.ucalgary.ca/d2l/le/content/44213/viewContent/3109344/View

Lei, C., Aldous, I., Hartley, J. M., Thompson, D. L., Scott, S., Hanson, R., . . . Abbott, A. P. (2021). Lithium ion battery recycling using high-intensity ultrasonication. *Green Chemistry*. doi:10.1039/d1gc01623g

Lewis, M. (2019, August). *Wells, Wires, Wheels*. Retrieved from BNP Paribas: https://www.easy.bnpparibas.fr/professional-professional/wells-wires-and-wheels/

Lutsey, N., & Nicholas, M. (2019). *Update on electric vehicle costs in the United States through 2030.* Washington DC: International Council on Clean Transportation. Retrieved from https://theicct.org/sites/default/files/publications/EV_cost_2020_2030_20190401.pdf

Masson-Delmotte, V., Zhai, P., Pirani, A., Connors, S. L., Péan, C., Berger, S., . . . (eds.), B. Z. (2021). *IPCC, 2021: Summary for Policymakers. In: Climate Change 2021: The Physical Science Basis. Contribution of Working Group I to the Sixth Assessment Report of the Intergovernmental Panel on Climate Change.* Cambridge University Press. Retrieved from https://www.ipcc.ch/report/ar6/wg1/downloads/report/IPCC_AR6_WGI_SPM.pdf

Murphy, C., Mai, T., Sun, Y., Jadun, P., Muratori, M., Nelson, B., & Jones, R. (2021). *Electrification Futures Study: Scenarios of Power System Evolution and Infrastructure Development for the United States.* Golden, CO: National Renewable Energy Laboratory. Retrieved from https://www.nrel.gov/docs/fy21osti/72330.pdf

National Renewable Energy Lab. (2021, June 21). *Researchers Identify Near-Term Opportunity for Heavy-Duty Electric Trucks*. Retrieved from National Renewable Energy Lab: https://www.nrel.gov/news/program/2021/researchers-identify-near-term-opportunities-for-heavy-duty-trucks.html

National Renewable Energy Laboratories. (n.d.). *PV Watts*. Retrieved from PV Watts: https://pvwatts.nrel.gov/pvwatts.php

Natural Resouces Canada. (2020, December 22). *Photovoltaic potential and solar resource maps of Canada*. Retrieved from Natural Resouces Canada: https://www.nrcan.gc.ca/our-natural-resources/energy-sources-distribution/renewable-energy/solar-photovoltaic-energy/tools-solar-photovoltaic-energy/photovoltaic-potential-and-solar-resource-maps-canada/18366

Natural Resources Canada. (2021, February 28). *Electric Charging and Alternative Fuelling Stations Locator*. Retrieved from Natural Resources Canada: https://www.nrcan.gc.ca/energy-efficiency/energy-efficiency-transportation-and-alternative-fuels/electric-charging-alternative-fuelling-stationslocator-map/20487#/find/nearest?country=CA&fuel=ELEC

Natural Resources Canada. (n.d.). *Photovoltaic Potential and Solar Resource Maps of Canada*. Retrieved from Natural Resources Canada: https://open.canada.ca/data/en/dataset/8b434ac7-aedb-4698-90df-ba77424a551f

Needell, Z. A., McNerney, J., Chang, M. T., & Trancik, J. E. (2016, August 15). Potential for widespread electrification of personal vehicle travel in the United States. *Nature Energy*. doi:https://doi.org/10.1038/nenergy.2016.112

Olsen, M. L., Rea, J., Glatzmaier, G. C., Hardin, C., Oshman, C., Vaughn, J., . . . Ginley, D. S. (2016). Solar thermoelectricity via advanced latent heat storage. *AIP Conference Proceedings 1734* (pp. 050035-1 - 050035-8). AIP Publishing. doi:https://doi.org/10.1063/1.4949133

OXTO Energy. (2021). *Our Technology*. Retrieved from OXTO Energy: https://oxtoenergy.com/technology.html

PlugShare. (2021, February 28). *West Hills Towne Centre - DC Fast Electric Car Charging - 192 Stewart Green SW, Calgary, AB T3H 3C8, Canada - Gas Station - PlugShare*. Retrieved from PlugShare: https://www.plugshare.com/location/208543

PlugShare. (2021a, February 28). *Petro-Canada - DC Fast Electric Car Charging - 42148 AB-1, Calgary, AB T3Z 3J1, Canada - Gas Station - PlugShare*. Retrieved from PlugShare: https://www.plugshare.com/location/199659

Primus Power. (2021). *Primus Power - Product*. Retrieved from Primus Power: https://primuspower.com/en/product/

Rea, J. E., Glatzmaier, G. C., Oshman, C., Parilla, P. A., Siegel, N. P., Ginley, D. S., & Toberer, E. S. (2018). Techno-Economic Analysis of a Small Scale Solar Power Tower at Varied Locations. *AIP Conference Proceedings 2033 - SolarPACES 2017* (pp. 040034-1 - 040034-8). AIP Publishing. doi:https://doi.org/10.1063/1.5067070

Rea, J. E., Oshman, C., Hardin, C. L., Singh, A., Alleman, J., Glatzmaier, G., . . . Toberer, E. S. (2018). Experimental demonstration of a latent heat storage system for dispatchable electricity. *AIP Conference Proceedings 2033 - SolarPACES 2017* (pp. 090022-1 - 090022-8). AIP Publishing. doi:https://doi.org/10.1063/1.5067116

Reed, S., Sugo, H., & Kisi, E. (2018). High temperature thermal storage materials with high energy density and conductivity. *Solar Energy*, 307-314. doi:https://doi.org/10.1016/j.solener.2018.02.005

Reuters Staff. (2021, February 11). *EU told 1 million public EV charging stations needed by 2024*. Retrieved from Reuters: https://www.reuters.com/article/idUSL8N2KH2S2

Salk Institute. (2021, August 17). *Capturing Atmospheric Carbon Dioxide and Transforming It Into Industrially Useful Materials*. Retrieved from SciTech Daily: https://scitechdaily.com/capturing-atmospheric-carbon-dioxide-and-transforming-it-into-industrially-useful-materials/

Scherer, S. (2021, June 29). *Canada to ban sale of new fuel-powered cars and light trucks from 2035*. Retrieved from Reuters: https://www.reuters.com/world/americas/canada-ban-sale-new-fuel-powered-cars-light-trucks-2035-2021-06-29/

Schlossberg, T. (2021, July 29). *The Race for EV Parts Leads to Risky Deep-Ocean Mining*. Retrieved from Yale Environment 360: https://e360.yale.edu/features/the-race-for-ev-parts-leads-to-risky-deep-ocean-mining

Sepulveda, N. A., Jenkins, J. D., Sisternes, F. J., & Lester, R. K. (2018). The Role of Firm Low-Carbon Electricity Resources in Deep Decarbonization of Power Generation. *Joule*, 2403–2420. doi:https://doi.org/10.1016/j.joule.2018.08.006

Sharpe, B., Lutsey, N., Smith, C., & Kim, C. (2020). *Power Play: Canada's Role in the Electric Vehicle Transition.* Washington DC: International Council on Clean Transportation. Retrieved from https://www.pembina.org/reports/canada-power-play-zev-04012020.pdf

Sisson, P. (2021, June 14). *The Quest to Green an Empire of Mega-Warehouses*. Retrieved from Bloomberg CityLab: https://www.bloomberg.com/news/articles/2021-06-14/california-launches-new-war-on-warehouse-pollution?srnd=citylab

Smil, V. (2010, May 14). *Power Density Primer: Understanding the Spatial Dimension of the Unfolding Transition to Renewable Electricity Generation (Part V – Comparing the Power Densities of Electricity Generation)*. Retrieved from Master Resource: https://www.masterresource.org/smil-vaclav/smil-density-comparisons-v/

Stratmann, T., Soetaert, K., Kersken, D., & Oevelen, D. v. (2021). Polymetallic nodules are essential for food-web integrity of a prospective deep-seabed mining area in Pacifc abyssal plains. *Scientific Reports*(21). doi:https://doi.org/10.1038/s41598-021-91703-4

Sudeyko, D., & Greacen, D. (2017). *Drake Landing Solar Community An Analysis of Future Renewable Energy Systems.* University of Calgary. Retrieved from https://d2l.ucalgary.ca/d2l/le/content/44213/viewContent/2605056/View

Sugo, H., Kisi, E., & Cuskelly, D. (2013). Miscibility gap alloys with inverse microstructures and high thermal conductivity for high energy density thermal storage applications. *Applied Thermal Engineering*, 1345-1350. doi:https://doi.org/10.1016/j.applthermaleng.2012.11.029

Tesla Canada. (2021, February 28). *Supercharger | Tesla Canada*. Retrieved from Tesla Canada: https://www.tesla.com/en_CA/supercharger

Thomas, S. T., Shin, Y., Clair, J. J., & Noel, J. P. (2021). Plant-based CO2 drawdown and storage as SiC. *RSC Advances*(26). doi:10.1039/d1ra00954k

Thompson, D. L., Hartley, J. M., Lambert, S. M., Shiref, M., Harper, G. D., Kendrick, E., . . . Abbott, A. P. (2020). The importance of design in lithium ion battery recycling – a critical review. *Green Chemistry*(22), 7585-7603. doi:10.1039/D0GC02745F

Transport Canada. (2020, February 25). *Joint Statement by Transport Canada and the U.S. Department of Transportation on the Nexus between Transportation and Climate Change*. Retrieved from Tranposrt Canada: https://www.canada.ca/en/transport-canada/news/2021/02/joint-statement-by-transport-canada-and-the-us-department-of-transportation-on-the-nexus-between-transportation-and-climate-change.html

U.S. Department of Energy. (2020). *Energy Storage Grand Challenge Energy Storage Market Report 2020.* U.S. Department of Energy. Retrieved from https://www.energy.gov/sites/default/files/2020/12/f81/Energy%20Storage%20Market%20Report%202020_0.pdf

U.S. Department of Energy. (2021). *National Blueprint for Lithium Batteries 2021-2030.* U.S. Department of Energy. Retrieved from https://www.energy.gov/sites/default/files/2021-06/FCAB%20National%20Blueprint%20Lithium%20Batteries%200621_0.pdf

United Nations. (n.d.). *The 17 Goals*. Retrieved from United Nations Department of Economic and Social Affairs: https://sdgs.un.org/goals

Williams, J. H., Jones, R. A., Haley, B., Kwok, G., Hargreaves, J., Farbes, J., & Torn, M. S. (2020). Carbon-Neutral Pathways for the United States. *AGU Advances*. doi:https://doi.org/10.1029/2020AV000284

Willuhn, M. (2021, June 30). *From toothbrushes to saving the planet: How ultrasonic delamination could hold the key to battery recycling*. Retrieved from PV Magazine: https://www.pv-magazine.com/2021/06/30/from-toothbrushes-to-saving-the-planet-how-ultrasonic-delamination-could-hold-the-key-to-battery-recycling/

Zhou, C., Lee, Y. K., Yu, Y., Byun, S., Luo, Z.-Z., Lee, H., . . . In. (2021, August). Polycrystalline SnSe with a thermoelectric figure of merit greater than the single crystal. *Nature Materials*, 1-9. doi:https://doi.org/10.1038/s41563-021-01064-6

APPENDICES

Appendix A – Energy Calculations

An assumption was made that the site would be able to accommodate three EVs charging per hour, over a daily operating duration of 15 hours, operating 365 days a year, for an estimated throughput of 16,425 total vehicles charged annually.

EV Charging System - Vehicle Throughput		
Number of vehicles per hour	3	vehicles per hour
Daily Hours of Operation	15	Hours
Days per Year	365	Days
Total Vehicles Charged	16,425	Annually

(Note: Choveaux, 2021)

3 vehicles/hr * 15 hours/day * 356 days/year = 16,425 Total Vehicles Charged, Annually

The Tesla Model 3 82 kWh battery pack was used as a proxy for the average battery pack size (Lambert, 2020). An assumption was made that each vehicle was estimated to have an average depth of discharge of 80% of the battery pack. Charging 3 vehicles per hour would require a total energy requirement of 196.8 kWh per hour. With daily operations of 15 hours, total daily energy requirements were calculated as 2,952 kWh/day. Over the span of 365 days, total annual energy requirement was determined to be 1,077,480 kWh/yr.

EV Charging System Requirements		
Number of vehicles per hour	3	vehicles per hour
Size of battery pack	82	kWh
Depth of Discharge	80	%
Hourly Energy Demand	196.8	kWh
Daily Hours of Operation	15	hours
Daily Energy Requirements	2,952	kWh
Yearly Energy Requirements	1,077,480	kWh/yr

(Note: Choveaux, 2021)

3 vehicles/hour * 82kWh battery pack * 80% depth of discharge = 196.8 kWh Hourly Energy Demand

196.8 kWh Hourly Energy Demand * 15 Daily Hours of Operation = 2,952 kWh Daily Energy Requirements

2,952 kWh Daily Energy Requirements * 365 Days/Year = 1,077,480 kWh/yr Yearly Energy Requirements

Over the 15 hours of daily operation, the system was modeled to provide 6 hours of daytime charging, requiring 9 hours of storage capacity for both battery and STEALS storage systems. Daytime charging was calculated as 6 hours of operation multiplied by the hourly energy demand of 196.8 kWh, resulting in a solar PV array sizing of 1,181 kWh for daytime charging. The total capacity for the battery was calculated as 9 hours multiplied by the hourly energy demand of 196.8 kWh, resulting in a minimum battery capacity of 1,771 kWh. An adjustment must be made based on the overall efficiency of the battery pack, estimated as 85% efficient, to ensure adequate charging of the system, requiring a solar PV array of 2,084 kWh for battery charging, resulting in overall daily energy requirements of 3,265 kWh, including system losses.

Solar PV + Battery Storage System Specifications		
Daily Energy Requirements (including system losses)	3265	kWh
Solar PV Array - Daytime Charging	1181	kWh
Solar PV Array (Battery Charging)	2084	kWh
Battery Size (9 hour storage)	1771	kWh

(Note: Choveaux, 2021)

196.8 kWh Hourly Energy Demand * 6 Hours Daytime = 1181 kWh Solar PV Array - Daytime Charging

196.8 kWh Hourly Energy Demand * 9 Hours Storage *0.85 Efficiency = 1771 kWh Battery Size (9 hour storage)

196.8 kWh Hourly Energy Demand * 9 Hours Storage / 0.85 Efficiency = 2084 kWh Solar PV Array (Battery Charging)

1181 kWh Solar PV Array + 2084 kWh Solar PV Array = 3265 kWh Daily Energy Requirements (including system losses)

To determine system sizing requirements for the solar PV + STEALS system, a literature review was undertaken to determine comparable capacity factors for the given location of Medicine Hat, Alberta. Previous studies had provided information on capacity factors for the STEALS system for the location of Daggett, California (Glatzmaier, et al., 2017). Using PV

Watts, Daggett, CA was found to have a direct nominal solar irradiance of 7.90 kWh/m^2/day, producing a capacity factor of 25.2 for solar PV installations (National Renewable Energy Laboratories, n.d.). Given that the literature provided a higher capacity factor for the STEALS system on the order of 31.4-38.1 (Glatzmaier, et al., 2017), this information was then used to make a proxy estimate of the potential capacity factor for the STEALS system when located in Medicine Hat, Alberta.

Again, PVWatts was used to determine the direct nominal irradiance for Medicine Hat, Alberta of 4.91 kWh/m^2/day, with a capacity factor of 16.4 for a solar PV array (National Renewable Energy Laboratories, n.d.). Given these factors, it was determined that a STEALS system located in Medicine Hat, Alberta would provide a capacity factor ranging from 19.5 to 23.7.

Solar Resource and Capacity Factor - Medicine Hat, AB		
Solar PV	Daggett, CA	Medicine Hat, AB
Direct Nominal Irradiance	7.90kWh/m^2/day	4.91kWh/m^2/day
Capacity Factor	25.2	16.4
STEALS	Daggett, CA	Medicine Hat, AB
Direct Nominal Irradiance	7.90kWh/m^2/day	4.91kWh/m^2/day
Capacity Factor (Low)	31.4	19.5
Capacity Factor (High)	38.1	23.7

(Note: Choveaux, 2021)

(31.4 Capacity Factor / 7.90kWh/m^2/day) * 4.91kWh/m^2/day = 19.5

(38.1 Capacity Factor / 7.90kWh/m^2/day) * 4.91kWh/m^2/day = 23.7

To compare the systems, I used the US National Renewable Energy Laboratories System Advisor Model to model the solar PV plus battery energy storage system. I uploaded location and resource data for Medicine Hat, Alberta (Natural Resources Canada, n.d.) into the SAM modeling software. In the SAM modelling software a system design with a nameplate capacity of 810 kWdc with a DC to AC ratio of 1.2 and an inverter efficiency of 96% was used. The system model employed an array with 1-axis tracking, 0 tilt degrees and a 180° azimuth, generating a system with total losses of 12.6% (Choveaux, 2021a).

SAM - Solar PV + Battery - System Parameters

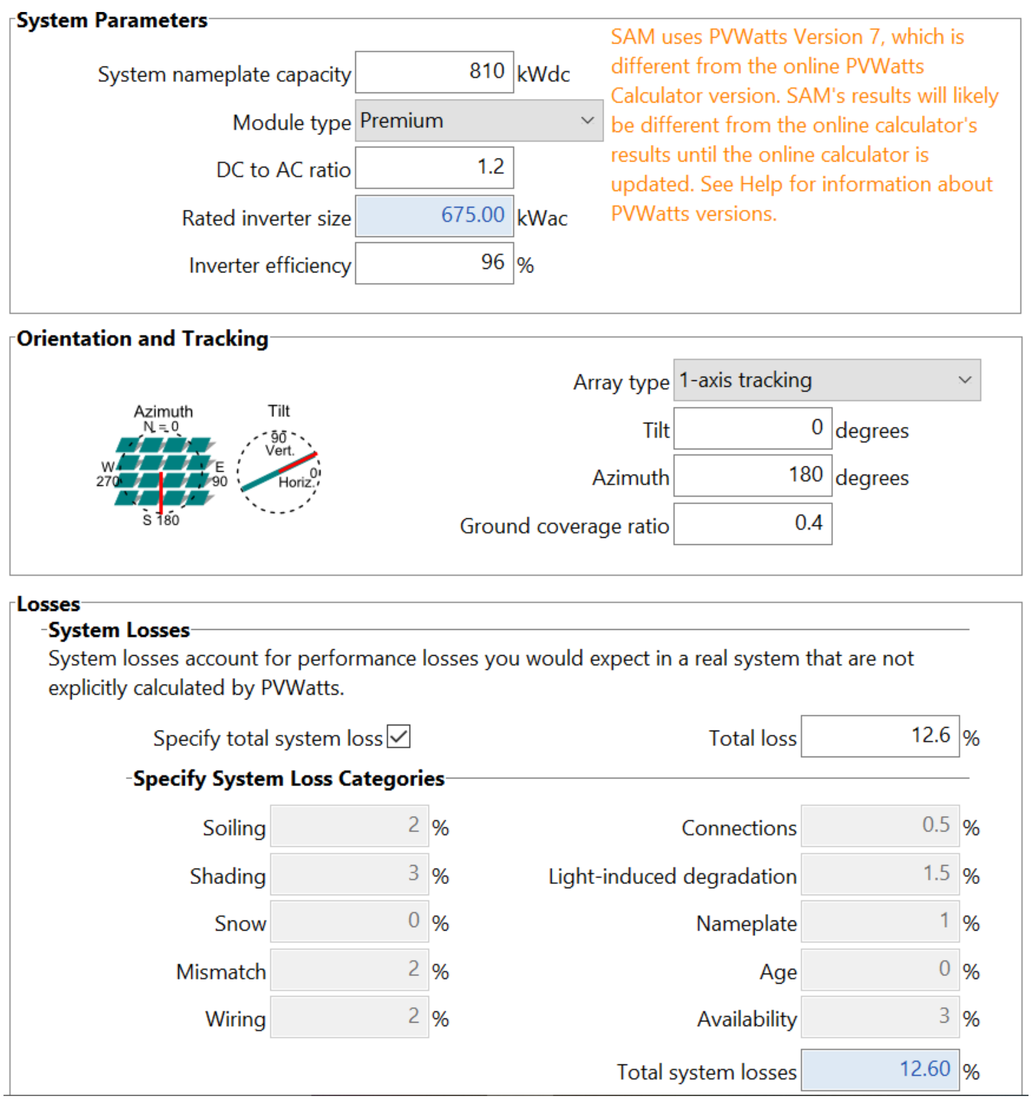

(Note: Choveaux, 2021a)

The solar PV component of the solar PV plus STEALS system was modelled using the SAM software. Given the difference in capacity factors for the different storage mediums, it was determined that a solar PV system plus STEALS would require a 300 kW solar PV array. This solar array would then be couple with a 450 kW STEALS storage system to produce requisite energy demand for EV charging.

In the SAM modelling software a solar PV array design with a nameplate capacity of 300 kWdc with a DC to AC ratio of 1.2 and an inverter efficiency of 96% was used. The system model employed an array with 1-axis tracking, 0 tilt degrees and a 180° azimuth, generating a system with total losses of 12.6% (Choveaux, 2021a).

SAM - Solar PV - System Parameters

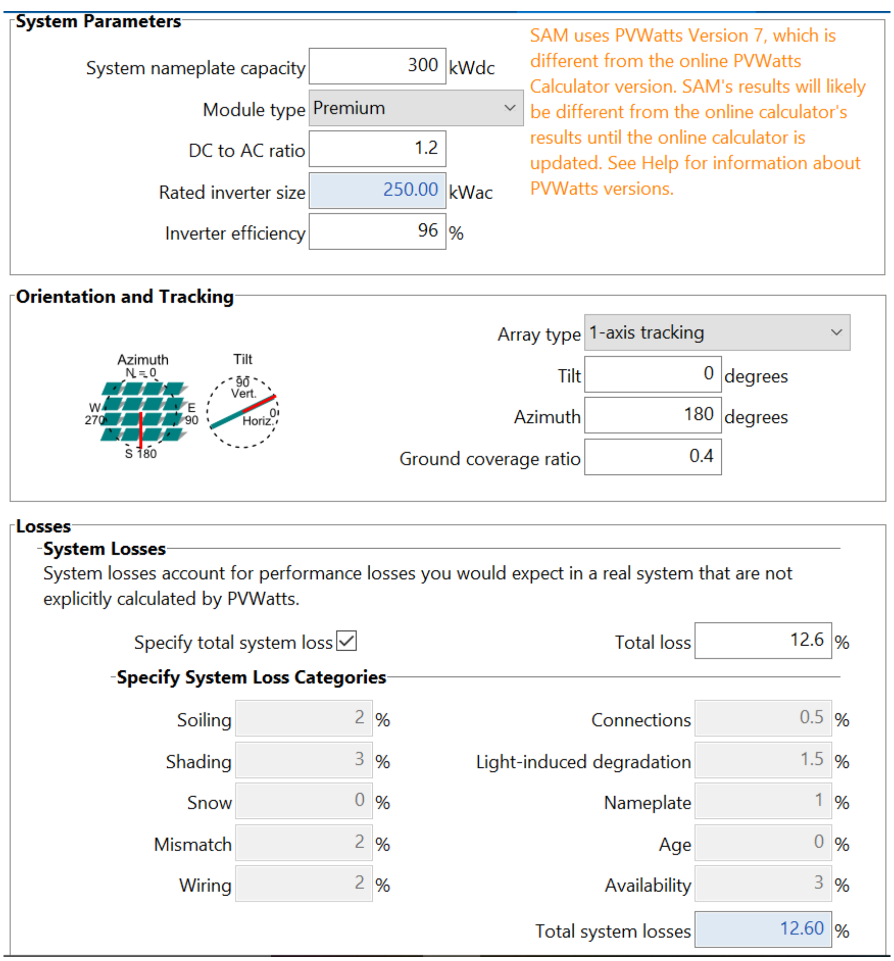

(Note : Choveaux, 2021a)

Appendix B – Environmental Calculations

To determine the amount of CO_{2e} emissions reductions from using renewable energy generation for EV charging, I looked at the total annual energy requirements for the system, 1,077,480 kWh/yr and the electricity grid displacement factor with renewable generation for the Alberta grid. I converted the total annual energy requirements to MWh/yr and then applied the electricity grid displacement factor for renewable generation of 0.53 tCO_{2e}/MWh (Government of Alberta, 2019), to determine a total annual emissions reduction of 571.06 tCO_{2e}/year displaced as a result of using renewable generation for EV charging.

Factor	t CO_2e/MWh	Description
Electricity grid displacement factor		
Electricity grid displacement with renewable generation	0.53	Applicable to projects displacing grid–electricity with renewable generation.
Electricity grid displacement factor with line loss applied		
Increased on-site grid electricity use (includes line loss)	0.57	Applicable for use in projects that increase electricity usage in the project condition.
Reduction in grid electricity usage (includes line loss)	0.57	Applicable to energy efficiency projects resulting in decreased grid electricity usage in the project condition.
Distributed renewable displacement at point of use (includes line loss)	0.57	Applicable to projects displacing grid electricity with distributed renewable electricity generation at point of use.

2018 Electricity Grid Displacement Discussion Paper, calculation methodology is based on 2007 EDC Associates, Calculation of the Grid Emission Intensity Factor for Alberta.

(Note: Government of Alberta, 2019)

EV Charging System Requirements & Emissions Reductions		
Yearly Energy Requirements	1,077.48	MWh/year
Electricity Grid Displacement Factor	0.53	tCO_{2e}/MWh
Annual Emissions Reductions	571.06	Total tCO_{2e}/year

(Note: Choveaux, 2021)

1,077,480 kWh/yr/1,000 = 1,077.48 MWh/year

1,077.48 MWh/year * 0.53 tCO_{2e}/MWh = 571.06 Total tCO_{2e}/year

Appendix C – Economic Calculations

The total capacity for the battery was calculated as 9 hours multiplied by the hourly energy demand of 196.8 kWh, resulting in a minimum battery capacity of 1,771 kWh. Using an average cost estimate of $250/kWh installed, total battery costs determined to be $442,800. Assuming a battery replacement would be required after 10 years operations, LCOE for the solar PV plus battery energy storage system increased from 17.48 cents/kWh to 18.77 cents/kWh with the battery replacement factored in (Choveaux, 2021a).

Solar PV + Battery Storage System Specifications		
Daily Energy Requirements (incl system losses)	3265	kWh
Solar PV Array - Daytime Charging	1181	kWh
Solar PV Array (Battery Charging)	2084	kWh
Battery Size (9 hour storage)	1771	kWh
LCOE PV + Battery (no battery replacement)	17.48	cents/kWh
LCOE PV + battery (battery replacement year 10)	**18.77**	cents/kWh

(Note: Choveaux, 2021)

SAM - Solar PV + Battery - Monthly Energy Production, LCOE

Metric	Value
Annual energy (year 1)	1,202,053 kWh
Capacity factor (year 1)	16.9%
Energy yield (year 1)	1,484 kWh/kW
Levelized cost of energy	18.77¢/kWh

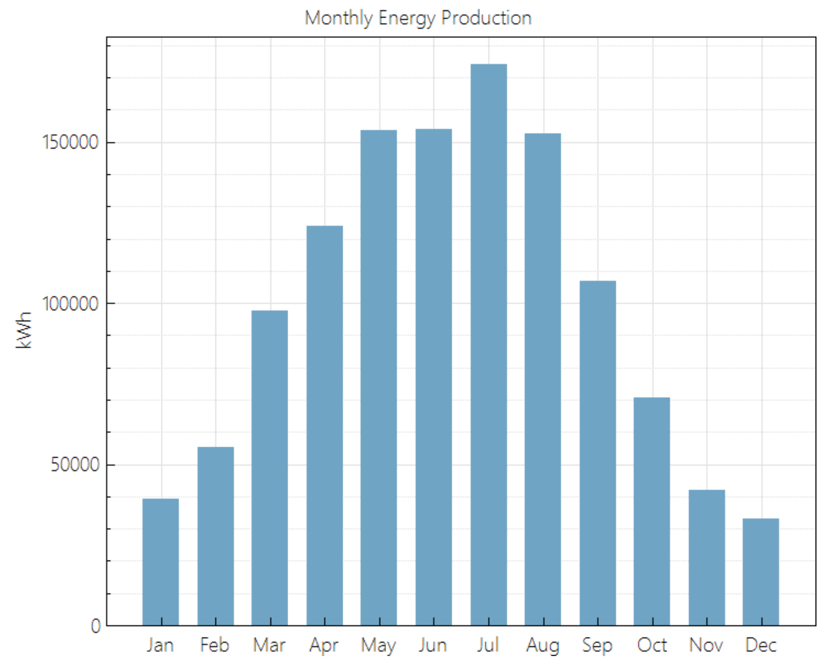

(Choveaux, 2021a)

The 300 kW solar PV array modeled in SAM had a LCOE of 14.67 cents/kWh.

SAM - Solar PV - Monthly Energy Production, LCOE

Metric	Value
Annual energy (year 1)	445,266 kWh
Capacity factor (year 1)	16.9%
Energy yield (year 1)	1,484 kWh/kW
Levelized cost of energy	14.67¢/kWh

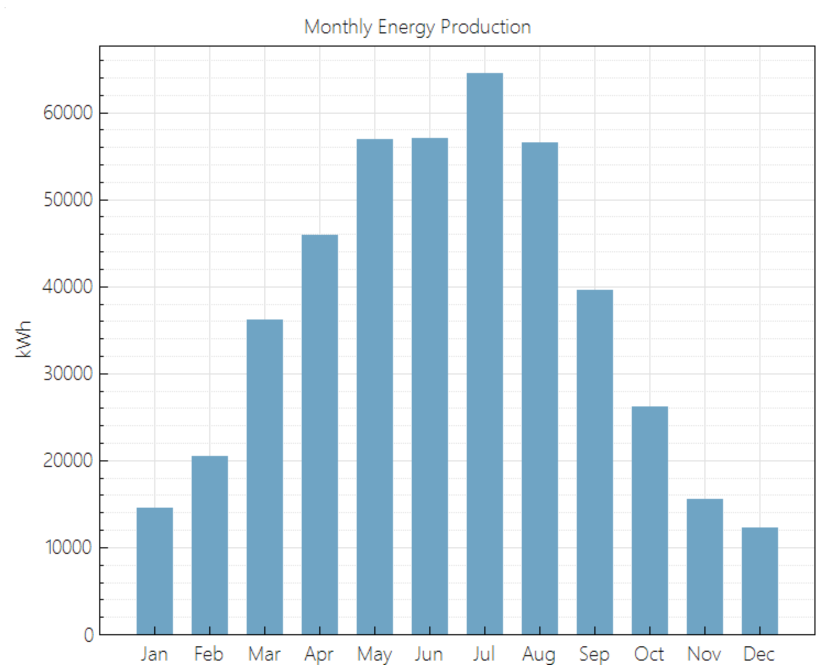

(Note: Choveaux, 2021a)

A literature review found that the high-end LCOE for a STEALS system to be 11.9 cents/kWh. Utilizing the high-end capacity factor of 23.7 for the Medicine Hat location, the STEALS component of the system had a LCOE of 19.13 cents/kWh, producing a total weighted average LCOE for the solar PV plus STEALS system design of 17.35 cents/kWh, producing a lower LCOE than the solar PV plus battery system.

Table 11 - Solar PV + STEALS Storage System Specifications

Solar PV + STEALS Storage System Specifications		
Solar PV Array	300	kW
STEALS system (9hr storage)	450	kW
LCOE PV	14.67	cents/kWh
LCOE STEALS	19.13	cents/kWh
Wgt Avg LCOE PV + STEALS	**17.35**	cents/kWh

(Note: Choveaux, 2021)

Appendix D – System Modeling Figures

SAM - Solar PV + Battery - System Parameters

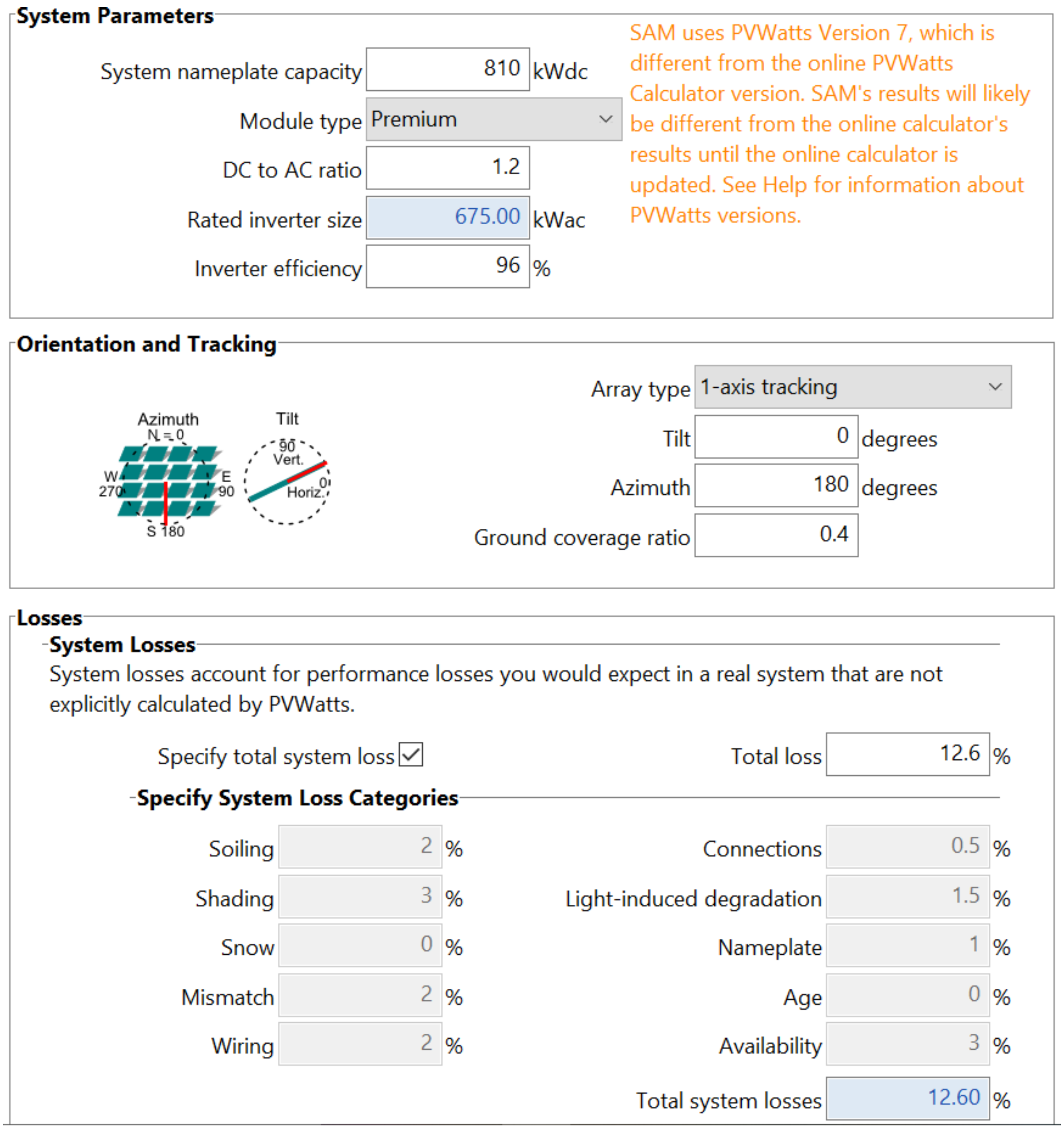

(Note: Choveaux, 2021)

SAM - Solar PV + Battery - Monthly Energy Production, LCOE

Metric	Value
Annual energy (year 1)	1,202,053 kWh
Capacity factor (year 1)	16.9%
Energy yield (year 1)	1,484 kWh/kW
Levelized cost of energy	18.77¢/kWh

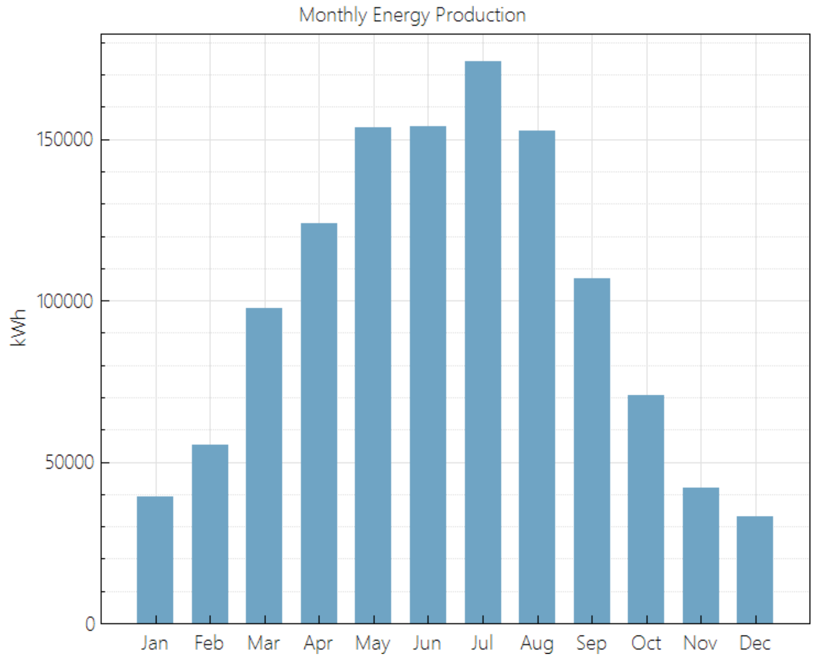

(Note: Choveaux, 2021)

SAM - Solar PV - System Parameters

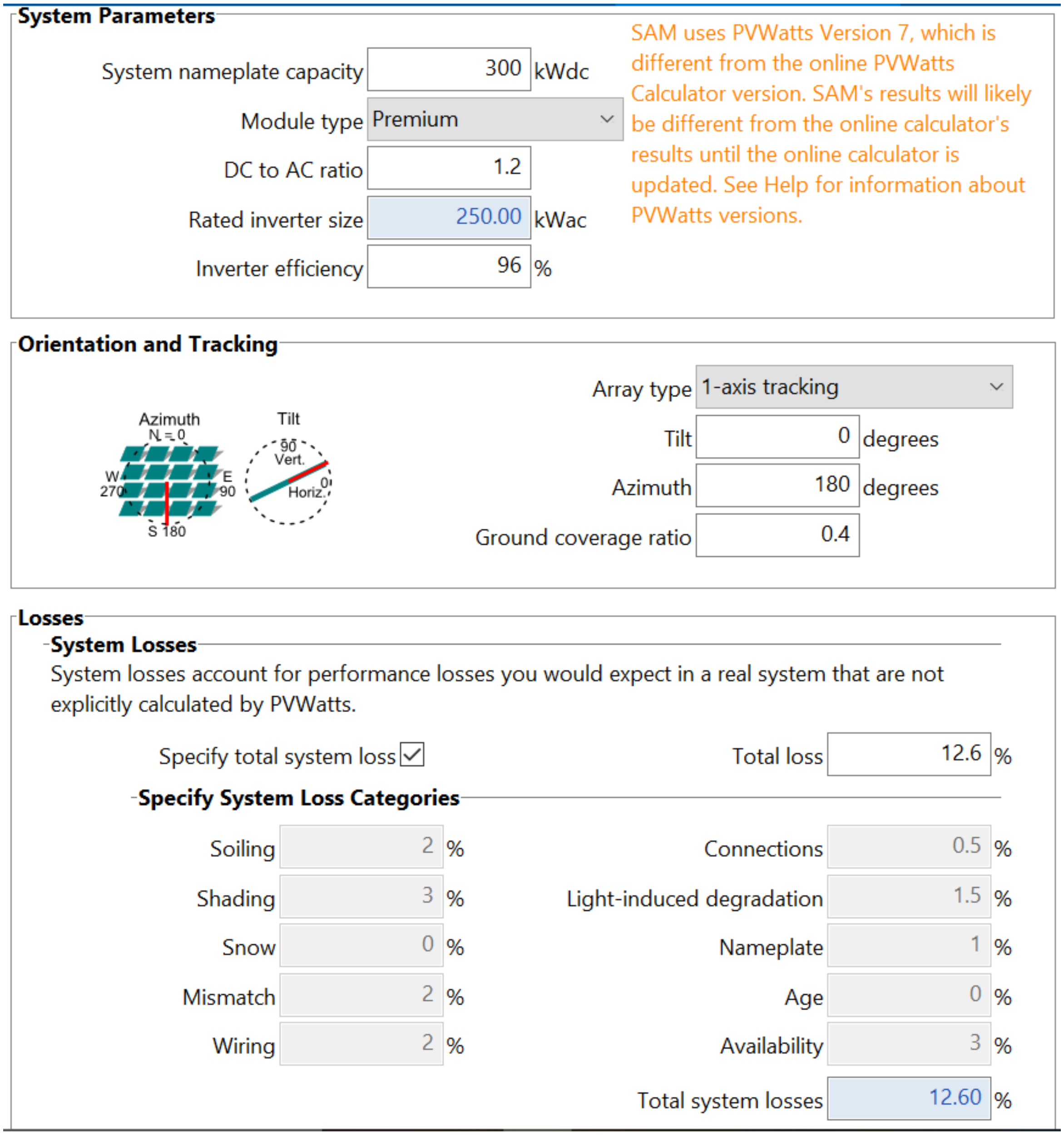

(Note: Choveaux, 2021)

SAM - Solar PV - Monthly Energy Production, LCOE

Metric	Value
Annual energy (year 1)	445,266 kWh
Capacity factor (year 1)	16.9%
Energy yield (year 1)	1,484 kWh/kW
Levelized cost of energy	14.67¢/kWh

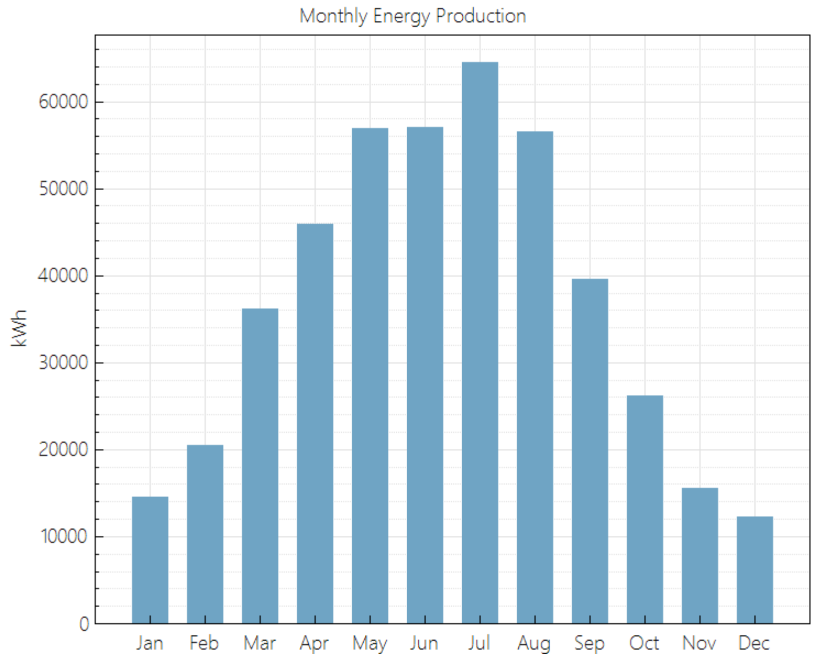

(Note: Choveaux, 2021)

Appendix E – PVWatts Solar Irradiance, Capacity Factor

PVWatts – Daggett, California - Solar Irradiance, Capacity Factor

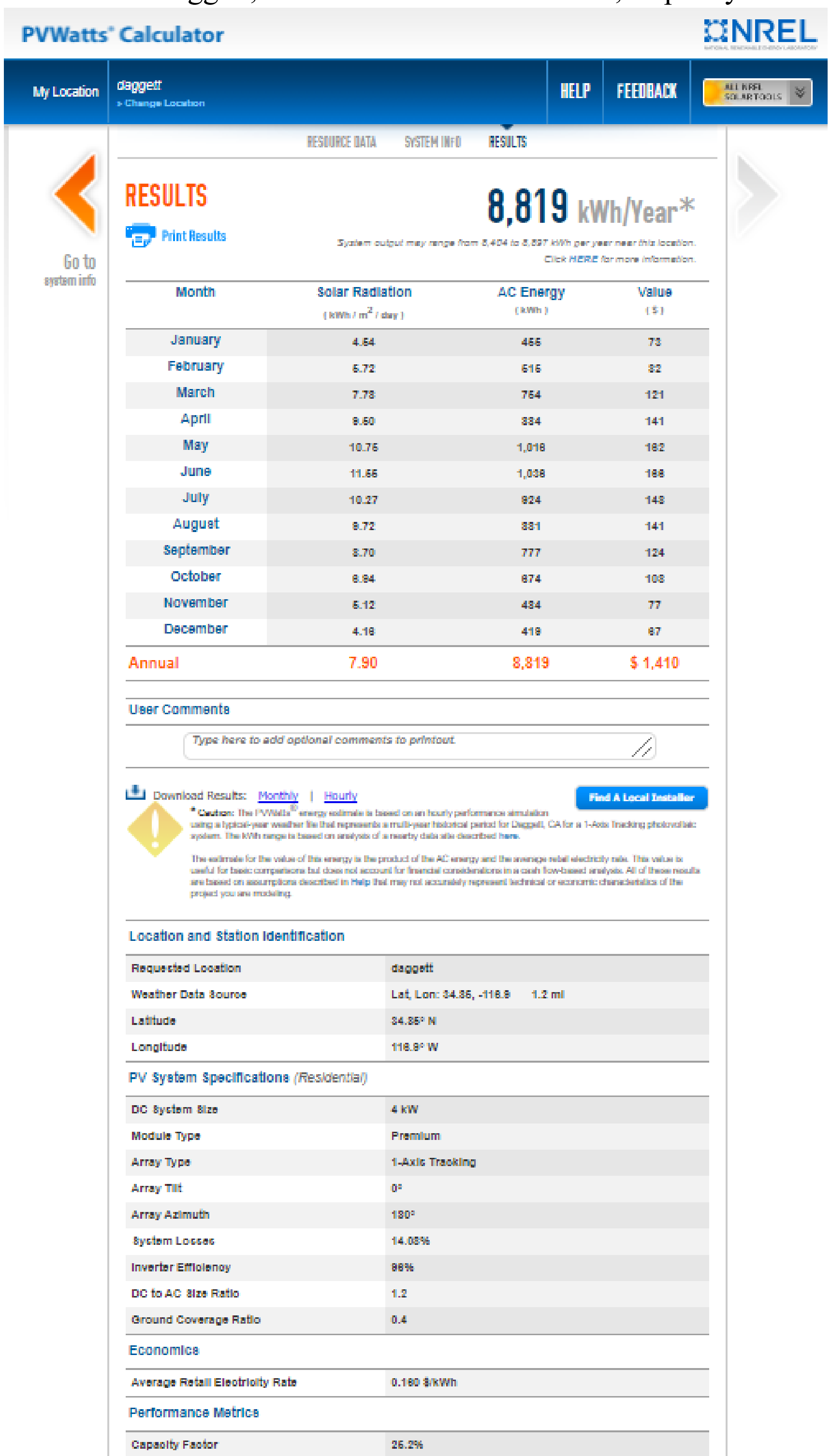

PVWatts® Calculator

My Location | daggett | > Change Location | HELP | FEEDBACK

RESOURCE DATA | SYSTEM INFO | RESULTS

Go to system info

RESULTS

Print Results

8,819 kWh/Year*

System output may range from 8,404 to 8,897 kWh per year near this location.
Click HERE for more information.

Month	Solar Radiation (kWh / m² / day)	AC Energy (kWh)	Value ($)
January	4.64	466	73
February	5.72	516	82
March	7.78	764	121
April	8.60	884	141
May	10.76	1,016	162
June	11.66	1,038	166
July	10.27	924	148
August	8.72	881	141
September	8.70	777	124
October	6.84	674	108
November	5.12	484	77
December	4.18	419	67
Annual	7.90	8,819	$ 1,410

User Comments

Type here to add optional comments to printout.

Download Results: Monthly | Hourly

Find A Local Installer

* Caution: The PVWatts® energy estimate is based on an hourly performance simulation using a typical-year weather file that represents a multi-year historical period for Daggett, CA for a 1-Axis Tracking photovoltaic system. The kWh range is based on analysis of a nearby data site described here.

The estimate for the value of this energy is the product of the AC energy and the average retail electricity rate. This value is useful for basic comparisons but does not account for financial considerations in a cash flow-based analysis. All of these results are based on assumptions described in Help that may not accurately represent technical or economic characteristics of the project you are modeling.

Location and Station Identification

Requested Location	daggett
Weather Data Source	Lat, Lon: 34.85, -116.8 1.2 mi
Latitude	34.85° N
Longitude	116.8° W

PV System Specifications *(Residential)*

DC System Size	4 kW
Module Type	Premium
Array Type	1-Axis Tracking
Array Tilt	0°
Array Azimuth	180°
System Losses	14.08%
Inverter Efficiency	96%
DC to AC Size Ratio	1.2
Ground Coverage Ratio	0.4

Economics

Average Retail Electricity Rate	0.160 $/kWh

Performance Metrics

Capacity Factor	25.2%

(Note: National Renewable Energy Lab, 2021)

PVWatts – Medicine Hat, Alberta - Solar Irradiance, Capacity Factor

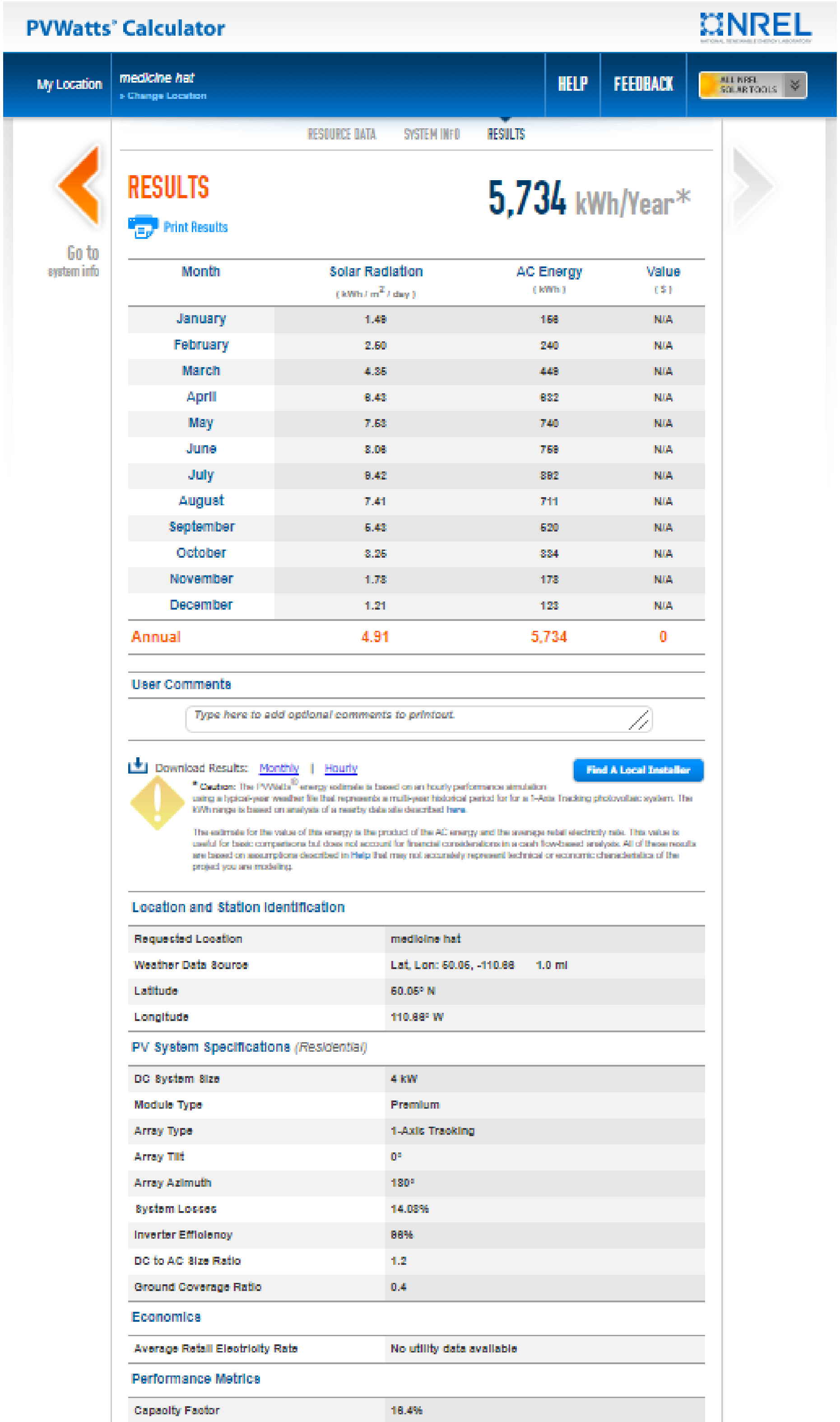

PVWatts® Calculator

NREL

My Location | medicine hat
» Change Location

HELP | FEEDBACK | ALL NREL SOLAR TOOLS

RESOURCE DATA | SYSTEM INFO | RESULTS

Go to system info

RESULTS

Print Results

5,734 kWh/Year*

Month	Solar Radiation (kWh / m² / day)	AC Energy (kWh)	Value ($)
January	1.49	168	N/A
February	2.60	240	N/A
March	4.36	448	N/A
April	6.43	632	N/A
May	7.53	740	N/A
June	8.06	769	N/A
July	8.42	882	N/A
August	7.41	711	N/A
September	5.43	520	N/A
October	3.26	334	N/A
November	1.78	173	N/A
December	1.21	123	N/A
Annual	4.91	5,734	0

User Comments

Type here to add optional comments to printout.

Download Results: Monthly | Hourly

Find A Local Installer

* Caution: The PVWatts® energy estimate is based on an hourly performance simulation using a typical-year weather file that represents a multi-year historical period for for a 1-Axis Tracking photovoltaic system. The kWh range is based on analysis of a nearby data site described here.

The estimate for the value of this energy is the product of the AC energy and the average retail electricity rate. This value is useful for basic comparisons but does not account for financial considerations in a cash flow-based analysis. All of these results are based on assumptions described in Help that may not accurately represent technical or economic characteristics of the project you are modeling.

Location and Station Identification

Requested Location	medicine hat
Weather Data Source	Lat, Lon: 50.05, -110.66 1.0 mi
Latitude	50.05° N
Longitude	110.66° W

PV System Specifications *(Residential)*

DC System Size	4 kW
Module Type	Premium
Array Type	1-Axis Tracking
Array Tilt	0°
Array Azimuth	180°
System Losses	14.08%
Inverter Efficiency	96%
DC to AC Size Ratio	1.2
Ground Coverage Ratio	0.4

Economics

Average Retail Electricity Rate	No utility data available

Performance Metrics

Capacity Factor	16.4%

(Note: National Renewable Energy Laboratories, n.d.)